International Journal of Digital Earth

ISSN: 1753-8947 (Print) 1753-8955 (Online) Journal homepage: www.tandfonline.com/journals/tjde20

Modeling the impacts of governmental and human responses on COVID-19 spread using statistical machine learning

Binbin Lin, Yimin Dai, Lei Zou & Ning Ning

To cite this article: Binbin Lin, Yimin Dai, Lei Zou & Ning Ning (2024) Modeling the impacts of governmental and human responses on COVID-19 spread using statistical machine learning, International Journal of Digital Earth, 17:1, 2434651, DOI: 10.1080/17538947.2024.2434651

To link to this article: https://doi.org/10.1080/17538947.2024.2434651

Published online: 09 Dec 2024.

INTERNATIONAL JOURNAL OF DIGITAL EARTH
2024, VOL. 17, NO. 1, 2434651
https://doi.org/10.1080/17538947.2024.2434651

Modeling the impacts of governmental and human responses on COVID-19 spread using statistical machine learning

Binbin Lin[a], Yimin Dai[b], Lei Zou[a]* and Ning Ning[b]*

[a]Department of Geography, Texas A&M University, College Station, TX, United States; [b]Department of Statistics, Texas A&M University, College Station, TX, United States

ABSTRACT

Understanding the impacts of governmental and human responses on the pandemic control is imperative for forecasting pandemic spread under various responsive scenarios and guiding localized interventions before pharmaceutical interventions are available. This study analyzed multiple data sets, including social media, mobility, policy evaluations, and COVID-19 infection reports, to delineate the interactions between governmental and human responses and COVID-19 spread in the United States in 2020 when vaccinations were unavailable. The contributions are (1) uncovering the spatiotemporal variations in governmental and human responses during COVID-19; (2) developing a statistical machine learning algorithm that incorporates spatiotemporal dependencies and temporal lag effects to model the relationships between governmental and human responses and the pandemic spread; (3) dissecting the impacts of human responses on the pandemic across space and time. Results reveal that the determinants of COVID-19 health impacts transitioned from human mobility during the initial outbreak phase to both human mobility and stay-at-home policies during the rapid spread phase, and ultimately to the compound of human mobility, stay-at-home policies and the public awareness in the full-blown phase. These findings furnish guidance for policymakers in implementing adaptive and phased strategies.

ARTICLE HISTORY
Received 16 August 2024
Accepted 19 November 2024

KEYWORDS
Bayesian model; COVID-19; human responses; spatiotemporal; geospatial data

1. Introduction

The COVID-19 pandemic, which emerged in 2020 and persisted for over three years, has profoundly impacted human society, posing significant threats to human health, disrupting social relationships, and devastating the economy (Li et al. 2020; Subramanian, He, and Pascual 2021). During the pandemic, governments worldwide implemented diverse policies to control the spread of the coronavirus. Meanwhile, individuals within different regions exhibited varying perceptions of the risks associated with COVID-19 and displayed divergent behaviors in response to the virus and adherence to relevant policies. These non-pharmaceutical governmental and human responses have played a crucial role in containing the pandemic during the absence of pharmaceutical interventions such as vaccinations, as evident in prior studies (Agusto et al. 2023; Hadjidemetriou et al. 2020;

CONTACT Lei Zou lzou@tamu.edu 205D Computing Service Annex, 3147 TAMU, College Station, TX 77843, USA; Ning Ning patning@tamu.edu 450G Blocker, 3257 TAMU, College Station, TX 77843, USA
*Lei Zou and Ning Ning both are corresponding authors

Liu et al. 2021; Manzira, Charly, and Caulfield 2022a; Kraemer et al. 2020; Wellenius et al. 2021). However, existing research has primarily focused on detecting the impacts of one or a limited scope of governmental and human responses to the COVID-19 spread, which overlooks the complexity in practical scenarios and may lead to the misinterpretation of the effectiveness of these responses. It is necessary to consider the compounding impacts of governmental and human responses simultaneously when modeling the pandemic's spread.

Modeling the compounding and evolving effects of governmental and human responses on COVID-19's health impacts has two main challenges: data availability and model complexity. Traditionally, data describing the dynamics of governmental and human responses to real-world events can be obtained through surveys. However, conducting large-scale surveys over an extended period is both time-consuming and financially burdensome, making it difficult to track human responses in near real-time. Recent technological advances have provided new opportunities for monitoring human responses to the pandemic. Geospatial big data, e.g. web application data (Rovetta and Bhagavathula 2020; Tsao et al. 2021) and sensor-based mobility data (Gao et al. 2020; Vinceti et al. 2020), offer rich information that can be used to delineate various dimensions of human behaviors, such as the strictness of COVID-19 related policies, public perceptions, and human mobility during the pandemic.

The second challenge is the model complexity. The impacts of diverse governmental and human responses to COVID-19 are intricately intertwined (Chen, Feng, and Gu 2022; Galea, Riddle, and Kaplan 2010), evolving over time, unevenly dispersed across space, and spatiotemporal dependent (Li et al. 2022). These intricacies necessitate an advanced model capable of comprehending the high dimensional spatiotemporal data, incorporating the spatial dependence and time lag effects in the human responses' impacts, and effectively capturing the spatiotemporal varied effects of governmental and human responses on COVID-19 spread. Despite the pressing need for such models, there remains a substantial gap in the development and application of advanced spatiotemporal models to fully address the intricacies of the human-COVID-19 system (Lin et al. 2024a). Conventional statistical models face challenges in handling high-dimensional data and uncovering interconnected relationships due to their limited capacity to capture complex patterns in such data. Deep learning models require large datasets to train vast model parameters and explain relationships among variables. Analyses at the administrative unit level are based on aggregated data, which have limited data points and are insufficient for training robust deep learning models. The emergence of statistical machine learning models (Sugiyama 2015) facilitates the ability to interpret relationships based on small-size datasets, providing opportunities to model the complex impacts of governmental and human responses on COVID-19 spread accurately at the administrative unit level.

This study analyzed the governmental and human responses, i.e. stay-at-home policies, public awareness and sentiment toward COVID-19, and human mobility, as well as their effects on COVID-19 health impacts in the U.S. at the state level. Considering that the first COVID-19 vaccination was released on December 14, 2020, this study chose the year 2020 as the focus period, which was before the widespread availability of vaccines, to assess the effects of non-pharmaceutical governmental and human responses on the pandemic control. The objectives of this study are threefold: (1) to reveal the spatiotemporally varied governmental and human responses during the COVID-19 pandemic in the U.S. using data from social media, web applications, and smartphone sensors; (2) to develop a statistical machine learning model that incorporates spatiotemporal dependence and time lag effects for relationship detection; (3) to unravel the impacts of governmental and human responses on the pandemic's health outcomes across time and space. The overarching hypothesis posits that stay-at-home policies and human mobility have a greater contribution to controlling the spread of COVID-19 compared to public awareness and sentiment. To test the hypothesis, we develop a novel Bayesian approach for modeling multiple correlated time series data that incorporates linear trend, seasonal, cyclical, and regression components. This method effectively captures spatial dependence between response and covariates while simultaneously

detecting time lag effects. It can automatically handle variable selection in high-dimensional datasets with complex patterns while preventing overfitting. Additionally, it provides a clear interpretation of the effects of different components.

The contributions include that (1) the developed framework and indices can be applied to observe governmental and human responses to other events like natural disasters and decipher their effects on human health; (2) we develop a novel statistical machine learning algorithm capable of modeling the spatially and temporally evolved interactions among various variables; (3) the knowledge gained from this study could provide an insightful understanding of governmental and human responses' impacts on COVID-19 spread and inform decision-making and policymaking for pandemic control.

2. Background

2.1. Spatiotemporal COVID-19 modeling

The COVID-19 pandemic had an unequal impact on different regions and populations throughout its progression partially due to the diverse, localized intervention strategies and responding behaviors. It is crucial to understand how COVID-19 has spread across different locations and over time to inform intervention strategies mitigating the uneven effects of future pandemics. Spatiotemporal modeling has emerged as a critical tool for achieving a detailed and accurate understanding of disease transmission patterns.

Epidemiological models are widely applied in modeling and predicting the spread of COVID-19, such as the Susceptible-Infected-Recovered (SIR) compartment model (Chen et al. 2020; Ma et al. 2024; Wangping et al. 2020). The SIR model divides a population into susceptible, infected, and recovered compartments. Through an ordinary differential equation (ODE) system to describe the dynamics and flows between the compartments, the SIR model can portray the pandemic spread by estimating important metrics such as the basic reproduction number (R_0) (Altmann 1995). However, this model assumes homogeneous dynamics across geographic areas, which does not reflect the spatial heterogeneity of the pandemic's spread and impacts. To address this limitation, researchers have developed spatial SIR-type models that consider spatial interactions between locations. For example, Hatami et al. (2022) developed a spatial Susceptible-Exposed-Infectious-Recovered (SEIR) model, incorporating a distance model describing pairwise relationships between studied locations with a traditional SEIR model. Another study by Hou et al. (2021) developed a human mobility flow-augmented stochastic SEIR model, applying an unsupervised machine learning algorithm to partition a county into multiple distinct subregions based on observed human mobility flow data. Ionides, Ning, and Wheeler (2022) and Ning and Ionides (2023) considered metapopulation systems characterized by strong dependence through time within a single unit and relatively weak interactions between units.

Spatial statistical regression models offer another approach to modeling the dynamics of epidemic spread. The Geographically and Temporally Weighted Regression (GTWR) model (Fotheringham, Crespo, and Yao 2015) is an extension of the Geographically Weighted Regression (GWR) model that incorporates temporal weighting. By allowing for the identification of local variations in the relationship between predictive variables and the response variable over time and space, the GTWR model has been successfully applied to estimate and forecast the spatial and temporal dynamics of COVID-19 spread in various regions (Chen et al. 2021; Fu and Zhai 2021). Similarly, the spatial error model (Wong and Li 2020), spatial lag model (Hafner 2020), and spatial vector autoregression model have been used to model the spread of COVID-19 while accounting for the effects of spatially structured errors and spatial dependence. Researchers have also developed novel methods to incorporate spatial and temporal features into COVID-19 prediction. Dlamini, Simelane, and Nhlabatsi (2022) conducted Bayesian network-based spatial predictive modeling to delineate the dynamics of COVID-19 spread. This model considers proximity referral health

facilities, churches, and shopping facilities as spatial variables. Incorporating spatial variables with daily traffic data and the proportion of youth, this model effectively identified COVID-19's potential geographic spread and the underlying influencing factors in Eswatini. Ak et al. (2022) constructed a structured Gaussian process model integrating spatial (geographical coordinates and location-specific demographic information) and temporal features (the day, month, and year information of the reported case counts) to forecast the outbreak of COVID-19.

2.2. Governmental and human responses to COVID-19

The COVID-19 pandemic has been acknowledged as a global crisis by the World Health Organization. Given the swift worldwide transmission of COVID-19 and the absence of an effective vaccine or treatment for this newly emerged infectious disease during its first outbreak, governmental and human responses have emerged as one of the primary strategies to mitigate the spread of COVID-19 in 2020.

Public health policies were one commonly adopted strategy to mitigate the transmission of COVID-19. In China, for example, the government implemented the zero-COVID-19 policy, employing large-scale testing, contact tracing technology, nationwide mask-wearing, and mandatory isolation of infected individuals to control the pandemic (Burki 2020). In the U.S., California became the first state to enforce a stay-at-home or shelter-in-place order. In March 2020, the New York City public school system, the largest in the U.S. with 1.1 million students, shut down, while Ohio mandated the closure of restaurants and bars. The effectiveness of COVID-19 control policy measures has been assessed. Liu et al. (2021b) conducted a study using panel regression to estimate the impact of 13 categories of COVID-19-related policies on reducing transmission across 130 countries from January to June 2020. Their findings revealed a strong positive correlation between strict policies such as school closures and internal movement restrictions and a decreased COVID-19 reproduction number. Another study conducted by Dainton and Hay (2021) examined the effects of COVID-19 lockdown policies on changes in human mobility utilizing Google Mobility data from five contiguous public health units in the Greater Toronto Area in Ontario, Canada, between March 1, 2020, and March 19, 2021. The study also assessed the subsequent impact of human mobility changes on the effective reproduction number of COVID-19, R_0, using Pearson correlation. The results indicated that, with enhanced lockdown measures, human mobility in York decreased significantly, particularly in retail, transit stations, and workplaces, leading to a reduced R_0 after 14 days.

The public perception of COVID-19 is another factor shaping residents' adherence to recommended policies and personal protective behaviors, such as wearing masks and practicing proper hand hygiene, ultimately leading to distinct spatiotemporal patterns of COVID-19 transmission. Cinarka et al. (2021) conducted a study using Google search volumes for COVID-19 symptoms as indicators of public awareness in Turkey, Italy, Spain, France, and the United Kingdom. The dynamic conditional correlation analysis method was employed to explore the relationships between Google search volumes and the COVID-19 spread. The findings revealed that the Google search volumes for symptoms such as fever, cough, and dyspnea were closely correlated with new COVID-19 cases during the initial outbreak of the pandemic. Jun, Yoo, and Lee (2021) utilized Google's relative search volume (RSV) as an indicator of public awareness regarding COVID-19 and employed a vector autoregression model to investigate its association with new COVID-19 cases in 37 countries in the Organization for Economic Cooperation and Development (OECD). The results demonstrated an association between increased public awareness and a heightened interest in COVID-19 testing. Agusto et al. (2023) employed ordinary differential equations to estimate the impact of public sentiment on the spread of COVID-19 in Australia, Brazil, Italy, South Africa, the United Kingdom, and the U.S. between January and June 2020. Public sentiments (both positive and negative) were evaluated using COVID-19-related tweets from Twitter (rebranded as X

in July 2023). The findings indicated that positive public sentiments were associated with a reduction in disease burden within the community.

Practically, the transmission of COVID-19 is influenced by numerous types of governmental and human responses simultaneously. Detecting the impacts of a portion of governmental and human responses on COVID-19 spread oversimplifies the interactions and may lead to the misinterpretation of the effectiveness of these responses. Therefore, accurate pandemic spread modeling necessitates considering the compounding impacts of government policies and various public reactions.

2.3. High-dimensional spatiotemporal statistical modeling

High-dimensional spatiotemporal challenges arise when dealing with data that involve both space and time, and where there are a large number of variables, locations, and time points. In recent years, there have been several statistical advances in addressing these challenges.

One direction is to use regularization methods such as Lasso (Tibshirani 1996) or Elastic Net (H. Zou and Hastie 2005), which can reduce the number of variables by assigning small coefficients to irrelevant variables. These methods can also identify important variables and their interactions. Another solution is dimension reduction which aims to reduce the number of variables in the data, while still capturing the relevant information. Principal component analysis (Zou, Hastie, and Tibshirani 2006; Ning and Ning 2024), factor analysis (Bhattacharya and Dunson 2011; Pati et al. 2014), and wavelet-based methods (Clyde, Parmigiani, and Vidakovic 1998) are examples of dimension reduction techniques that have been applied to spatiotemporal data. These methodological advancements have substantially contributed to addressing the difficulties associated with analyzing high-dimensional and spatiotemporal data. As a result, there have been improvements in model development and predictions to resolve questions across various disciplines, such as environmental science, epidemiology, and climate modeling. Nonetheless, methodologies capable of simultaneously managing high-dimensional issues and spatiotemporal data remain scarce, primarily due to the intricate nature of feature selection tasks within complex structures.

The advances in the Bayesian structural time series (BSTS) model bring opportunities to address the challenges in high dimensional spatiotemporal statistical modeling. BSTS (Scott and Varian 2014) is a statistical technique to select features, forecast temporal trends, and infer causal impacts (Brodersen et al. 2015). The model is designed to work with time series data by incorporating various components, such as seasonality, trends, or auto-regression. It can also accommodate external regressors, which makes it possible to quantify the impacts of regressors on the response. Recent literature (Sung 2023; Zhang and Fricker 2021) has utilized the BSTS model to analyze COVID-19 data. Based on BSTS, the Multivariate BSTS (MBSTS) (Qiu, Jammalamadaka, and Ning 2018; Ning and Qiu 2023) was proposed as a novel tool for inferring and predicting multiple correlated time series. Qiu, Jammalamadaka, and Ning (2018) demonstrates that the MBSTS model provides better prediction accuracy compared to the univariate BSTS model, the autoregressive integrated moving average with regression (ARIMAX) model, and the multivariate ARIMAX (MARIMAX) model. Also, MBSTS can select features from a pool of contemporary predictors while simultaneously training models for each time series, which reduces over-fitting and eliminates unessential or misleading predictors. In other words, MBSTS can choose distinct predictor sets for each target time series for each Markov chain Monte Carlo iteration from high-dimensional data.

In the human-pandemic interactions, high-dimensional governmental and human responses exhibit intricate inter-dependencies and have compounded impacts on epidemics. In this scenario, the MBSTS model, due to its inherent capability for feature selection and over-fitting prevention, is suitable for detecting the compounded effects of governmental and human responses on pandemic transmission.

3. Data

Figure 1 illustrates the conceptual framework describing the hypothesized effects of governmental and human responses on COVID-19 health impacts with a time lag effect. The stay-at-home policies, public awareness and sentiment toward COVID-19, and human mobility were selected as governmental and human responses in this study (Table 1). Section 3 outlines the data collection and processing methods employed to measure governmental and human responses and COVID-19 health impacts.

3.1. COVID-19 risk perceptions

We designed several indices based on Twitter data to capture COVID-19 risk perceptions and their changes at the state-level. Twitter, one of the most popular social media, provides users with a platform to share their experiences, feelings, and opinions about events through short messages (tweets) (Zou et al. 2019). In 2023, Twitter was renamed and branded as X, and the remainder of this article uses Twitter to avoid confusion. Compared with the survey, Twitter data are an invaluable resource for researchers due to two advantages. Firstly, with 450 million monthly active users as of 2023, Twitter data are more representative of a larger population than survey data. Secondly, Twitter data can be used to quantitatively monitor human perceptions and behaviors during COVID-19 in the near-real time (Bogdanowicz and Guan 2022), whereas conducting surveys is time-consuming which makes it difficult to track public perceptions promptly. However, it is worth mentioning that Twitter data, like many other social media platforms, are inherently biased towards younger, well-educated, and wealthier urban populations (Blank 2017). Analyzing Twitter data without considering demographic biases might overlook the behavior of certain social groups and lead to unfair estimations.

To track demographically unbiased public awareness and sentiment toward COVID-19, we conducted the Twitter data mining framework, as depicted in Figure 2. First, we collected all geotagged tweets from the U.S. in 2020 using the Twitter Academic Application Programming Interface (API). Non-human generated tweets and tweets from organizational accounts, which were irrelevant to

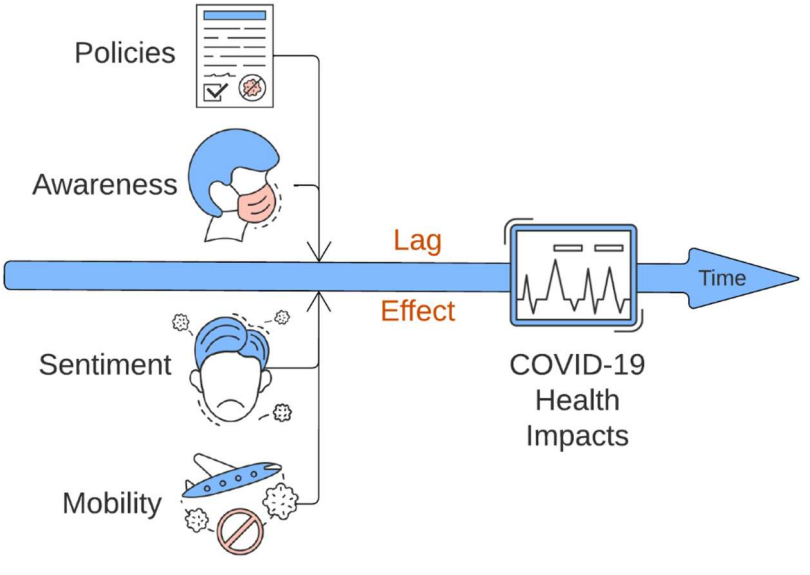

Figure 1. The conceptual framework describing the hypothesized effects of governmental and human responses on COVID-19 health impacts with a time lag effect.

Table 1. Overview of variables used for governmental and human responses.

Category	Index name	Index meaning	Data source
COVID Risk Perception-Public awareness	Ratio Adjusted by Demographics (RAD)	The demographically unbiased percentages of COVID-19 related Tweets	Twitter/X
COVID Risk Perception-Public sentiment	Negative-Sentiment Adjusted by Demographics (N-SAD) and Positive-Negative-Sentiment Adjusted by Demographics (*P*-SAD)	The demographically unbiased percentages of Twitter/X users expressing overall negative (N-SAD) and positive (*P*-SAD) emotions toward COVID-19	Twitter/X
Mobility	Human mobility in Driving, Transit, and Walking	Relative mobility volume based on baseline volume in different transportation types	Apple Human Mobility Reports
COVID-19 Policies	Stringency Index (SI)	The strictness of stay-at-home COVID-19 policies	Oxford COVID-19 Government Response Tracker (OxCGRT)

public perceptions, were removed by methods delineated in (Lin et al. 2022). A total of 255,291,871 geotagged tweets were retrieved. Second, we set a list of COVID-19-related keywords based on existing literature (Alqurashi, Alhindi, and Alanazi 2020; Banda et al. 2021), i.e. *covid*, *virus*, *2019-ncov*, *sars-cov-2*, *coronavirus*, *ncov*, *n95*, *social distancing*, *lockdown*, *quarantine*, *pandemic*, *epidemic*, *pneumonia*, and *confirmed cases*, to identify tweets relevant to the pandemic. A total of 3,954,468 tweets (1.55%) were identified as COVID-19-related. Third, we calculated three matrics to indicate risk perceptions. The percentage of COVID-19-related tweets overall geotagged tweets is defined as the Ratio index to represent public awareness toward COVID-19 (Lin et al. 2022). In terms of public sentiment toward COVID-19, we estimated users' sentiment toward COVID-19 (negative, neutral, or positive) based on the sentiment of all COVID-19-related tweets they posted (Lin et al. 2024b). The M3 (multimodal, multilingual, and multi-attribute) model proposed by Wang et al. (2019) was employed to detect the demographics of users including age and gender based on users' screen names, usernames, profile images, and biographies. The M3 model achieves an accuracy of 0.81 for gender recognition and 0.42 for age recognition on the English tweet data set, exceeding other available models (Morgan-Lopez et al. 2017; Vashisth and Meehan 2020). Finally, the positive and negative Sentiments Adjusted by Demographics (P-SAD and N-SAD) index and Ratio Adjusted by Demographics (RAD) index were computed using the post-stratification method based on the difference between the demographic structure of Twitter users and the general population, as suggested in (Lin et al. 2024b). The N-SAD and P-SAD indexes represent the demographically unbiased percentages of Twitter users expressing overall negative and positive emotions toward COVID-19, respectively. The RAD index quantifies the proportion of tweets concerning COVID-19 among all tweets after correcting Twitter users' demographic biases. All risk perception indexes can be computed at different spatial and temporal scales.

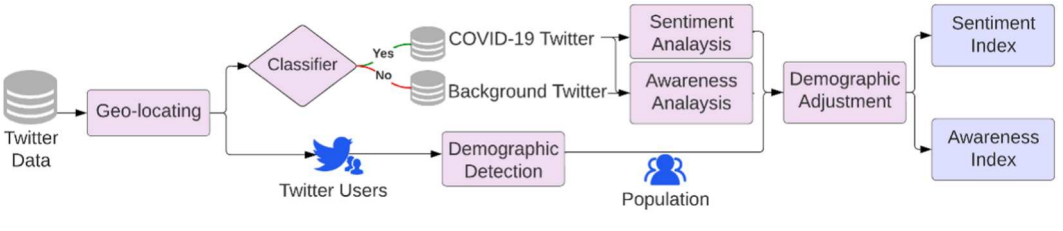

Figure 2. Framework of Twitter data mining for demographically-unbiased assessments of public awareness and sentiment toward COVID-19.

3.2. Mobility

This study collected daily Apple mobility data in the U.S. at the state level in 2020 to assess human mobility in different modes, namely driving, walking, and public transit. The Apple human mobility data track the mobility volume change in driving, walking, and taking public transit at multiple administrative levels, e.g. global, country, state, and county (https://covid19.apple.com/mobility). The data were derived from Apple Maps users and reported as the relative volume based on the baseline volume, which was the direction requests received per country/region, sub-region, or city on January 13th, 2020. Although the dataset only includes Apple Maps users, Apple has a significant market share in the US, with millions of active users. This large sample size provides a robust dataset to monitor spatiotemporal changes in human mobility during significant events like COVID-19 (Kurita et al. 2021; Nagy et al. 2023), although it is not perfectly representative of the entire population. It is worth noting that Apple is no longer offering mobility trends reports as of April 2022.

3.3. COVID-19 policies

The Oxford COVID-19 Government Response Tracker (OxCGRT) using the scorecard method, offers a systematic estimation of the stringency of COVID-19 policies implemented by various countries since January 1st, 2020. Hale et al. (2021) compiled a comprehensive set of policies and assigned scores to each policy, with higher scores indicating more stringent measures. These policies were categorized into 23 indicators based on their thematic focus. The Stringency Index (SI) selected in this investigation quantifies the strictness of stay-at-home COVID-19 policies by incorporating nine indicators, namely school closures, workplace closures, restrictions on public events, limitations on gathering size, public transport closures, stay-at-home requirements, restrictions on internal movement, restrictions on international travel, and public information campaigns. The SI scale ranges from 0 to 100, with higher values indicating more stringent measures. For this study, we collected daily SI data at the state level in the U.S. throughout 2020. Although policy evaluations are included in this study, we recognize that policies like lockdown orders were not uniformly followed during COVID-19. Incorporating both policies and public responses provides a realistic understanding of how humans perceive policies differently, how disparities in their perception affect behaviors, and the resultant health consequences.

3.4. COVID-19 cases

To assess the health implications of COVID-19, we utilized the case rate as a quantitative measure, which represents the proportion of confirmed cases per 100,000 individuals within the population. The cumulative confirmed cases in the U.S. in 2020 were collected from the publicly accessible database maintained by the Center for Systems Science and Engineering (CSSE) at Johns Hopkins University (Dong, Du, and Gardner 2020). Population data were sourced from the United States Census, and estimates were based on data as of April 1st, 2020. The resulting case rate values ranged from 0 to 105, with higher values indicating a more pronounced impact on public health attributed to COVID-19.

4. Methods

The MBSTS model is a generalized version of various structural time series models, leveraging Bayesian selection techniques through Markov Chain Monte Carlo (MCMC) methods to select among a set of contemporary predictors. This model offers flexibility in choosing different components, allowing users to construct complex structures. To address delayed effects,

we incorporated the time lag effect into the MBSTS model. This section first provides an overview of the MBSTS model, followed by a detailed description of the modified MBSTS with the time lag effect algorithm.

4.1. The MBSTS model

The MBSTS model is a general time series model constructed as the sum of trend $\mu(t)$, season $\tau(t)$, cycle $\omega(t)$, and regression $\xi(t)$ components with $t \in \{1, \ldots, T\}$ being the time index, as follows:

$$Y(t) = \mu(t) + \tau(t) + \omega(t) + \xi(t) + \epsilon(t), \quad \epsilon(t)\ i.i.d.\ \sim N_M\Big(0,\ \sum \epsilon\Big) \tag{1}$$

where $Y(t) = \{Y_m(t)\}_{m=1}^{M}$ is the M-dimension outcome vectors. All components are assembled independently, with each component yielding an additive contribution. The MBSTS model allows each $Y_m(t)$ for $m \in \{1, \ldots, M\}$ to have its specific formula. For instance, for predicting two-dimension outcome vectors, the first time series may encompass the trend, season, and regression components, while the second time series may only have the trend component. The model training is conducted over all M time series incorporating the correlations through $M \times M$-dimensional covariance associated with the error term $\epsilon(t)$.

The specification of the trend component ($\mu(t)$) in a time series model depends on both the characteristics displayed by the analyzed series and any available prior knowledge. If the series consistently demonstrates either an upward or downward movement, incorporating a slope or drift into the trend model could be suitable. This results in a more comprehensive model compared to the local linear trend model. In this generalized version, the slope remains stationary rather than random, and the model can be expressed in the following form:

$$\mu(t+1) = \mu(t) + \tilde{\delta}(t) + \tilde{\mu}(t), \quad \tilde{\mu}(t)\ i.i.d.\ \sim N_M\Big(0,\ \sum \mu\Big) \tag{2}$$

$$\tilde{\delta}(t+1) = \tilde{D} + \tilde{\rho}(\tilde{\delta}(t) - \tilde{D}) + \tilde{\nu}(t), \quad \tilde{\nu}(t)\ i.i.d.\ \sim N_M\Big(0,\ \sum \delta\Big) \tag{3}$$

Here, $\tilde{\delta}(t)$ and $\tilde{D}$ represent m-dimensional vectors. Specifically, $\tilde{\delta}(t)$ signifies the expected increase in $\mu(t)$ between time t and t + 1 to resemble a short-term slope at time t. In contrast, $\tilde{D}$ pertains to the long-term slope. This structural setup harmonizes short-term insights with long-term trends, resulting in a model that appropriately blends both types of information.

The second component of the model ($\tau(t)$) is responsible for capturing seasonality and is commonly expressed as follows:

$$\tau_m(t+1) = -\sum_{k=0}^{S_m-2} \tau_m(t-k) + \omega_m(t),\ \tilde{\omega}(t) = [\omega_1(t), \ldots, \omega_M(t)]^T\ i.i.d.\ \sim N_M\Big(0,\ \sum \tau\Big) \tag{4}$$

Here, S_m represents the number of seasons for the time-series $Y_m(t)$ for $m \in \{1, \ldots, M\}$, and the M-dimensional vector $\tau(t) = (\tau_1(t), \ldots, \tau_M(t))$ signifies their collective influence on the observed target time series $Y(t) = (Y_1(t), \ldots, Y_M(t))$. The MBSTS model accommodates diverse seasonal components with distinct periods for each target series $Y_m(t)$. For instance, it's possible to incorporate a seasonal component with $S_m = 7$ to capture the day-of-the-week effect for one target series, and $S_{m'} = 30$ to account for the day-of-the-month effect in another target series.

The third component of the series ($\omega(t)$) aims to capture cyclical effects. In economics, the term 'business cycle' refers to recurrent deviations around the long-term trajectory of the series that are not strictly periodic. A model encompassing a cyclical component can effectively replicate crucial features of the business cycle, such as robust autocorrelation, alternating phases, damping fluctuations, and null long-term persistence. A stochastic trend model, when applied to a seasonally

adjusted economic time series, may not adequately capture the series' short-term fluctuations on its own. However, by integrating a serially correlated stationary component, the model becomes equipped to account for these short-term movements, thereby encompassing the cyclical influence. The cycle component is defined as follows:

$$\omega(t+1) = \varrho\widehat{cos(\lambda)}\omega(t) + \varrho\widehat{sin(\lambda)}\omega*(t) + \tilde{k}(t), \quad \tilde{k}(t)\ i.i.d. \sim N_M\left(0, \sum\omega\right) \tag{5}$$

$$\omega*(t+1) = -\varrho\widehat{sin(\lambda)}\omega(t) + \varrho\widehat{cos(\lambda)}\omega*(t) + \tilde{k}*(t), \quad \tilde{k}*(t)\ i.i.d. \sim N_M\left(0, \sum\omega\right) \tag{6}$$

where ϱ, $\widehat{sin(\lambda)}$, and $\widehat{cos(\lambda)}$ are $M \times M$ diagonal matrices with diagonal entries equal to ϱ_{ii} (a damping factor for target series Y_i such that $0 < \varrho_{ii} < 1$), $sin(\lambda_{ii})$ where $\lambda_{ii} = 2\pi/q_i$ is the frequency with q_i being a period such that $0 < \lambda_{ii} < \pi$, and $cos(\lambda_{ii})$ respectively.

The regression component $\xi(t) = (\xi_1(t), \ldots, \xi_M(t))$ with static coefficients is written as Equation (7).

$$\xi_m(t) = \beta_m^T X_m(t) \tag{7}$$

Here, $\xi(t) = [\xi_{m,1}(t), \ldots, \xi_{m,d}(t)]^T$ is the collection of all elements in the regression component. For target series Y_m, $X_m(t) = [X_{m,1}(t), \ldots, X_{m,d}(t)]^T$ is the pool of predictors at time t, and $[\beta_{m,1}, \ldots, \beta_{m,d}]^T$ represents corresponding static regression coefficients. Regression analysis is a statistical methodology used to estimate relationships between dependent variables and independent variables, which are alternatively referred to as predictors, covariates, or features. That is, each time series has its specific d predictors that are different from those of other time series. The total number of different predictors for the M-dimensional time series is thus Md.

The MBSTS model can select important features while taking into account the spatial correlations among target time series by the spike and slab technique developed by George and McCulloch (1997) and Madigan and Raftery (Madigan and Raftery 1994) that has been widely used for dimension reduction (Jammalamadaka, Qiu, and Ning 2019; Ning and Ning 2024; Qiu, Jammalamadaka, and Ning 2020). Additionally, the model is equipped to infer the trend component $\mu(t)$, the seasonal component $\tau(t)$, and the cyclical component $\omega(t)$ via a posterior simulation algorithm as outlined by Durbin and Koopman (Durbin and Koopman 2002). Moreover, it enables the inference of covariance matrices associated with these components, namely, $\left(\sum\mu, \sum\delta, \sum\tau, \sum\omega\right)$ through an inverse Wishart distribution.

4.2. The MBSTS-TL algorithm

Although the MBSTS model is suitable for detecting the compounding effects of governmental and human responses on pandemic transmission, it is imperative to recognize that the influence of human responses on the epidemic may exhibit delayed effects. There is a need to modify the MBSTS model, which currently assumes that factors affect the target time series instantaneously, by incorporating time lag effects associated with governmental and human responses. This augmentation is critical for improving the model's capacity to faithfully capture real-world dynamics. Therefore, we propose a new Algorithm 1 named MBSTS-Time Lagged (MBSTS-TL) model. MBSTS-TL is designed to work with the MBSTS model for the spatiotemporal setting with a time lag of l_t. This model introduces a proper error metric for evaluation and hyper-parameter tuning. Effective hyper-parameter selection is crucial in spatiotemporal analysis. The hyper-parameter ρ denotes the trend effect as defined in Equation (3), while S represents the seasonal effect as defined in Equation (4). Additionally, ϱ and λ denote the damping factor and cyclic effect, respectively, as defined in Equation (6). The MBSTS model is a time series model that includes trend, seasonal, cycle, and regression $\xi(t)$ components. Each hyper-parameter controls its respective component. The trend effect ρ denotes that the local linear component at time $t+1$, $\tilde{\delta}(t+1)$, is equal to the

local linear component at time t, $\tilde{\delta}(t)\tilde{D}$, multiplied by ρ and added to $\tilde{D}$ with noise. The seasonal effect S indicates that the seasonal component $\tau(t+1)$ at time $(t+1)$ is equal to the sum of the seasonal components from time $t-S+2$ to time t. The damping factor and cyclic effect controls the iteration of cycle component from time $t+1$ to t. The novel error metric, denoted as $AE_{\rho,S,\varrho,\lambda}$ facilitates the tuning of hyper-parameters (ρ, S, ϱ, and λ) associated with the MBSTS model. It takes into account both temporal variations and spatial disparities. This methodology identified a diverse set of candidate parameters and selected the optimal one to enhance our model. This work represents the first attempt to provide an explicit hyper-parameter tuning method within the MBSTS framework.

To elaborate, we divide the time interval $[t^{start}, t^{end}]$ into non-overlapping K segments, creating a partition as follows: $\left[t_1^{start}, t_1^{end}\right]$, $\left[t_2^{start}, t_2^{end}\right]$, …, $\left[t_K^{start}, t_K^{end}\right]$. This partition allows us to evaluate model performance in distinct time stages, considering the error metric defined in Equation (8). Importantly, this time-based partitioning does not increase the computational complexity in the MBSTS model. Given that Markov chain Monte Carlo, an offline method, is employed, training the MBSTS model with all time-dependent data might lead to lengthy convergence times and require substantial computational resources. Our approach addresses this issue by allowing users to define time partitions that align with the evolving dynamics of events, such as the varying stages of the COVID-19 spread. For each MBSTS model corresponding to a partition segment, a smaller-scale Markov chain Monte Carlo is performed. This not only makes the process computationally feasible on personal computers but also adapts the model to the evolving nature of spatiotemporal phenomena.

Algorithm 1 The MBSTS-TL algorithm

INPUT: Covariate $X(t_k^{start}), \ldots, X(t_k^{end}-l_t)$ and outcome $Y(t_k^{start}+l_t), \ldots, Y(t_k^{end})$ for k $\in$ {1, …, K}.

Evaluation:

1. Training the k-th MBSTS model for k = 1, …, K, with hyper-parameter ρ, S, ϱ, and λ using

$X(t_k^{start}), \ldots, X(t_k^{end}-l_t)$ and $Y(t_k^{start}+l_t), \ldots, Y(t_k^{end})$.

2. One step prediction of $Y(t_k^{end})$ with $X(t_k^{end}-l_t)$ using the trained k-th MBSTS model with hyper-parameter ρ, S, ϱ, and λ. Denote the prediction as $\hat{Y}(t_k^{end})$, for k $\in$ {1, …, K}.

3. Compute the normalized absolute values of the differences between the true values $Y(t_k^{end}) = \{Y_m(t_k^{end})\}_{m=1}^M$ and its corresponding predicted values $\hat{Y}(t_K^{end}) = \{\hat{Y}_m(t_K^{end})\}_{m=1}^M$, i.e.

$$AE_{\rho,S,\varrho,\lambda}(l_t) = \left(\frac{\sum_{m=1}^M |\hat{Y}_m(t_1^{end}) - Y_m(t_1^{end})|}{M\ max_{m\in\{1,\ldots,M\}} Y_m(t_1^{end})}, \ \ldots, \ \frac{\sum_{m=1}^M |\hat{Y}_m(t_K^{end}) - Y_m(t_K^{end})|}{M\ max_{m\in\{1,\ldots,M\}} Y_m(t_K^{end})} \right) \quad (8)$$

Training:

1. Grid search for the optimal hyper-parameters ρ^*, S^*, ϱ^*, and λ^* in their user-defined spaces that yield the minimum $AE_{\rho,S,\varrho,\lambda}(l_t)$ for different l_t.

2. Generate regression coefficients $\beta_k = [\beta_{k,1}, \ldots, \beta_{k,d}]^T$ and its confidence interval (CI) for k $\in$ {1, …, K}.

OUTPUT: parameters β_k, its CI, and predictions $\hat{Y}^*(t_k^{end})$ for k $\in$ {1, …, K}, and error $AE_{\rho^*,S^*,\varrho^*,\lambda^*}(l_t)$.

The impacts of governmental and human responses to COVID-19 spread evolved across different stages of the pandemic. To capture the time-varying primary human responses for COVID-19 containment, the time interval of 53 weeks during the year 2020 was divided into three segments, as suggested in previous investigations (Kim, Zanobetti, and Bell 2021; Wu and Sha 2021): $\left[t_1^{start}, t_1^{end}\right] = [9, 22]$, $\left[t_2^{start}, t_2^{end}\right] = [23, 37]$, and $[t_3^{start}, t_3^{end}] = [38, 53]$, representing February 24th to May 31st, June 1st to September 13th, and September 14th to December 31st, 2020. These periods, corresponding to the onset of the outbreak, the phase of rapid spread, and the full-blown phase of the pandemic, were named as the initial outbreak, rapid spread, and full-blown periods, respectively. The hyper-parameters of ρ, S, ϱ, and λ in the Algorithm 1 are selected in the training process.

5. Results

5.1. Temporal trends of COVID-19 health impacts and governmental and human responses in the U.S.

Figure 3 illustrates the U.S. temporal trends of COVID-19 health impacts and governmental and human responses from week 3 to week 53 (mid-January to the end of December) in 2020. The case rate fluctuated from 0 to 69.62, characterized by three distinct stepwise increments. There were two minor ascensions of approximately 10 each, occurring between weeks 13 to 22 (late March to the end of May 2020) and weeks 23 to 37 (June to mid-September), as well as a rapid ascent to approximately 60 between weeks 38 to 47 (mid-September to late November). Subsequently, the case rate dynamically sustained itself around 60 between weeks 48 and 53 (late November to the end of December 2020). The risk awareness RAD index ranged from 0.01 to 5.21. It remained proximate to 0 before week 8 (mid-February 2020), after which it underwent a rapid ascent commencing in week 11 (mid-March), reaching its zenith in week 12, followed by a descent to 0.99 by week 23 (early June). Thereafter, it maintained values around 1.5. The policy evaluation SI index ranged from 0.31 to 79.45. Prior to week 9 (the end of February 2020), values remained below 5, but subsequent to week 10 (early March), a rapid ascent was observed, reaching its pinnacle at week 16 (mid-April), followed by a gradual descent. Values around 60 were sustained from week 25 (mid-June 2020) to week 53 (the end of December).

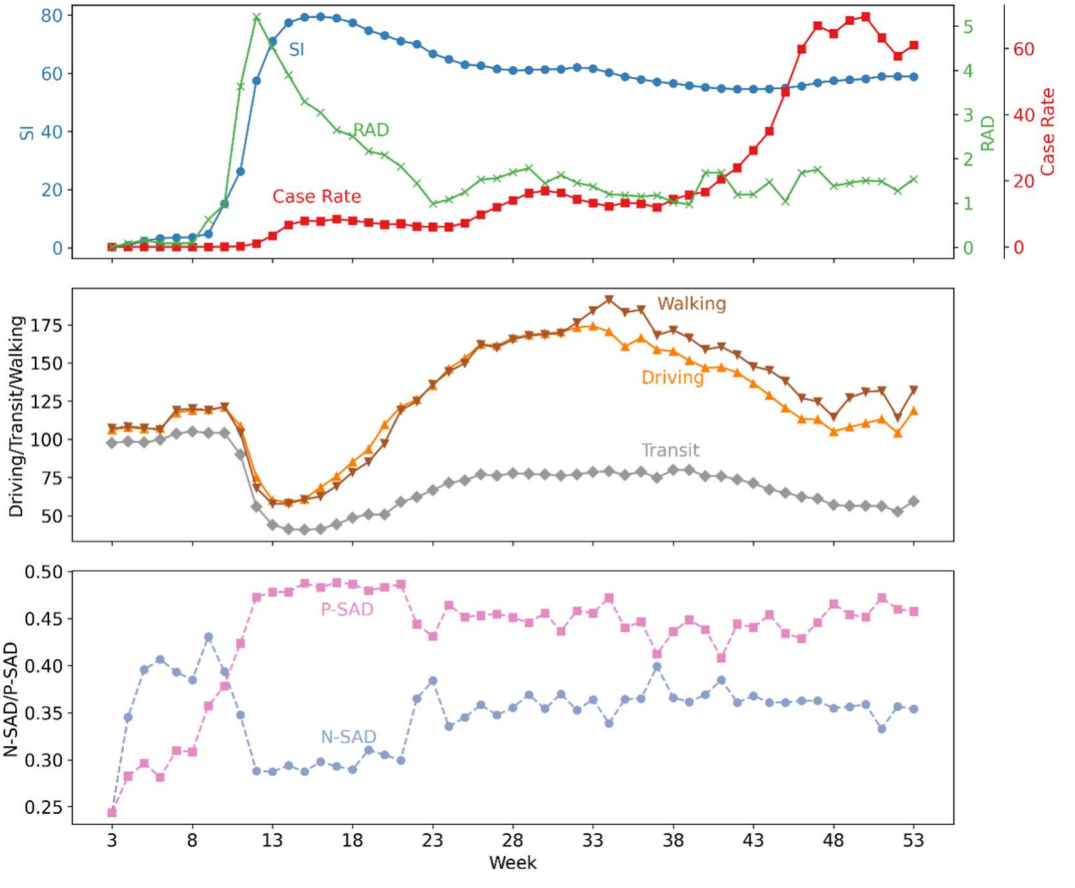

Figure 3. National temporal trends of COVID-19 health impacts and human responses.

Regarding the variations in human mobility, the walking Index ranged from 57.74 to 191.47, the driving Index ranged from 58.88 to 174.19, and the transit Index ranged from 40.75 to 80.04. These three indices exhibited similar trends, with each maintaining relatively stable values from weeks 3 to 10 (mid-January to early March 2020), at 110, 110, and 100, respectively. A decline was observed from week 11 (mid-March 2020), reaching respective minima in weeks 13 (the end of March), 14, and 15 (early April), followed by an ascent to their peaks from weeks 28 to 38 (early July to mid-September). Finally, they gradually decreased to approximately 125, 110, and 57 by weeks 48 to 53 (late November to the end of December 2020). In general, the trends for walking and driving exhibited a high degree of overlap, characterized by an early rapid decline, recovery, and surpassing of the normal baseline values. The usage of public transits exhibited a more pronounced initial decline compared to walking and driving, with subsequent recovery, and it did not return to the values observed in the normal status, maintaining an overall lower value.

For the characterization of sentiment, the N-SAD index ranged from 0.24 to 0.43. Prior to week 9 (late March 2020), it exhibited an upward trajectory, increasing from a minimum of 0.24 to a maximum of 0.43. Thereafter, a rapid decline ensued, reaching 0.29 by week 12 (mid-March 2020). From weeks 12 to 21 (mid-March to late May 2020), the index remained at around 0.3, subsequently stabilizing at approximately 0.35 from week 22 to week 53 (late May to the end of December). The P-SAD index ranged from 0.24 to 0.49. It underwent a rapid ascent from week 3 to week 12 (mid-January to mid-March 2020), increasing from 0.24 to 0.47, and subsequently maintained values around 0.47 from week 13 to week 21 (late March to late May), followed by values around 0.45 from week 22 to week 53 (late May to the end of December). Notably, during the initial 3 to 10 weeks (mid-January to early March 2020), corresponding to the period prior to the COVID-19 outbreak in the U.S., the proportion of Twitter users expressing negative sentiment towards the pandemic was higher than those with a positive sentiment. Conversely, after the initial outbreak, the proportion of users expressing negative sentiment rapidly declined, while those with positive sentiment exhibited a substantial increase. After week 11 (mid-March), the proportion of Twitter users with a positive sentiment consistently exceeded those with a negative sentiment.

5.2. Spatiotemporal disparities of COVID-19 health impacts and governmental and human responses

Figure 4 depicts the spatial disparities of COVID-19 case rates, SI index, and RAD index at the state level across three phases in 2020: the initial outbreak period, the rapid spread period, and the full-blown period.

During the initial outbreak period, the case rate ranged from 0 to 19, with New York state exhibiting the highest case rate. In the rapid spread period, case rates ranged from 1.06 in Vermont to 27.54 in Louisiana. States in the southern region of the United States, such as Florida (26.88), Arizona (25.11), and Mississippi (24.87), demonstrated notably higher case rates. In the full-blown period, case rates spanned from 8.68 in Vermont to 89.45 in North Dakota, with northern states like South Dakota (86.98), Wisconsin (68.90), and Wyoming (65.23) displaying higher case rates.

The policy SI index during the initial outbreak period ranged from 45.41 in North Dakota to 71.92 in Maine. States with relatively higher SI indices included Maryland (71.71), Kentucky (68.85), Delaware (68.81), New Mexico (68.66), and New York (68.27). Conversely, states with lower SI indices encompassed South Dakota (49.79), Arizona (51.75), and Utah (52.04). In the rapid spread period, the SI index varied from 43.98 in Oklahoma to 82.05 in New Mexico, with states like Maine (81.95), Hawaii (76.85), New York (74.03), and Kentucky (69.42) displaying higher SI indices. Lower SI indices were observed in states like North Dakota (46.04), South Dakota (47.62), and Missouri (48.14). In the full-blown period, the SI index ranged from 40.02 in Oklahoma to 76.61 in Hawaii. States with higher SI indices included New Mexico (74.85), New York (72.66), and Connecticut (66.27), while states with lower SI indices were South Dakota (41.31), Florida (43.03), and Alabama (43.52). Overall, New Mexico and New York maintained higher SI indices

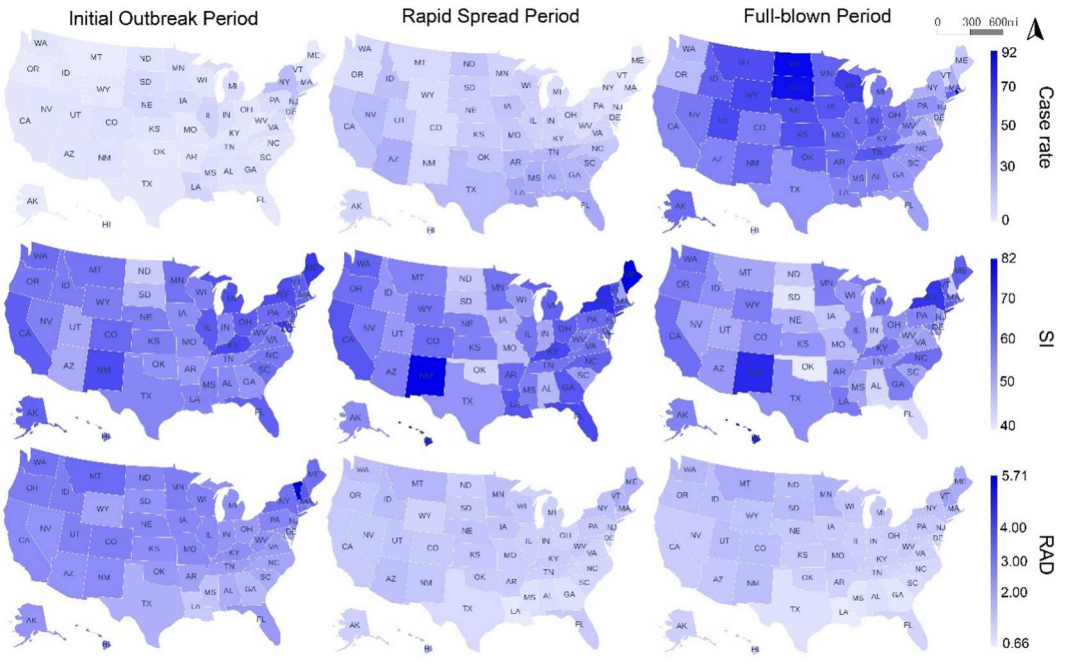

Figure 4. Spatiotemporal disparities of COVID-19 health impacts, SI and RAD.

throughout the three phases, suggesting stricter stay-at-home policies in these states. North Dakota and South Dakota consistently exhibited lower SI indices across the three phases, indicating more relaxed stay-at-home policies.

The risk awareness RAD index during the initial period ranged from 1.39 in Louisiana to 5.71 in Vermont, with other states such as New Hampshire (3.78) and Massachusetts (3.46) exhibiting higher RAD indices. Lower RAD indices were observed in states like Louisiana (1.39) and Mississippi (1.53). In the rapid spread period, the RAD index ranged from 0.69 in Louisiana to 2.10 in Vermont, with higher RAD indices in Hawaii (1.91) and Maine (1.91). Lower RAD indices were observed in Georgia (0.87) and Mississippi (0.88). In the full-blown period, the RAD index ranged from 0.66 in Louisiana to 2.31 in Vermont, with higher RAD indices in New Hampshire (2.13) and Montana (2.04). Lower RAD indices were observed in Georgia (0.76) and Mississippi (0.76). It is evident that Louisiana consistently exhibited lower RAD indices across all three phases, indicating lower levels of public awareness of the pandemic among Twitter users in that state.

Figure 5 illustrates the spatial disparities in human mobility categorized into three modes: Transit, Walking, and Driving at the state level during three distinct periods of the pandemic. Areas depicted in gray signify the unavailability of data. During the initial outbreak period, Transit usage ranged from 30.57 (Hawaii) to 107.85 (Mississippi). In addition to Hawaii, New York and Washington displayed lower Transit usage values of 32.43 and 34.51, respectively. In contrast, Alabama and Arkansas displayed higher Transit usage values of 97.18 and 95.93, respectively, along with Mississippi. Notably, Mississippi was the sole state with a Transit value exceeding 100, signifying a general reduction in Transit mobility across states due to the pandemic's impact. In the rapid spread period, Hawaii continued to exhibit the lowest Transit value (21.55), while Mississippi maintained the highest value (135.68). New York and Washington maintained lower Transit values of 39.19 and 42.87, respectively. This indicates that the impact of the pandemic on Transit mobility persisted longer in Hawaii, New York, and Washington. During the full-blown period, Transit ranged from 26.63 (Hawaii) to 109.97 (Mississippi). Alabama (101.86) and Arkansas (100.62) reported Transit values exceeding 100, and New Hampshire and South Carolina

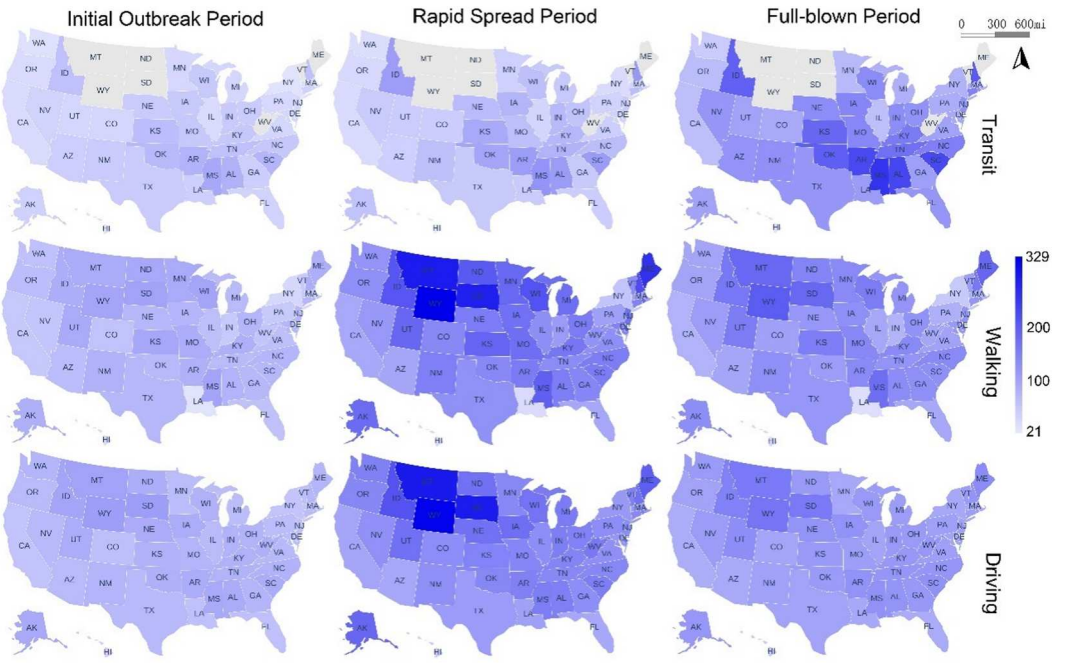

Figure 5. Spatiotemporal disparities of human mobility.

also recorded values surpassing 90. This suggests that only five states had Transit mobility nearly returned to pre-pandemic normalcy.

Walking and Driving mobility exhibited a similar spatiotemporal pattern. During the initial outbreak period, Driving ranged from 55.70 (Hawaii) to 121.68 (South Dakota), while Walking ranged from 30.79 (Louisiana) to 116.60 (South Dakota). In the rapid spread period, Driving ranged from 60.67 (Hawaii) to 324.86 (Wyoming). Walking ranged from 43.25 (Louisiana) to 328.53 (Wyoming). In addition to Louisiana, only Hawaii and New York reported values below 100, at 43.65 and 71.77, respectively. The remaining states exhibited values exceeding 100, with Wyoming, Montana, South Dakota, and Maine displaying notably high values. In the full-blown period, Walking ranged from 53.00 (Hawaii) to 212.64 (Wyoming), while Driving ranged from 64.63 (Hawaii) to 175.21 (Wyoming). Wyoming, Montana, South Dakota, and Maine continued to exhibit high Walking and Driving values.

Hawaii is the only state where Transit, Walking, and Driving values remained consistently below 100 in all three phases. This signifies that residents of Hawaii experienced the most significant impact on their human mobility due to the pandemic, and recovery over a year has proven challenging.

Figure 6 depicts the spatiotemporal disparities in public sentiment towards COVID-19 across three periods. The negative sentiment index (N-SAD) reached its lowest values in Vermont, with values of 0.25, 0.26, and 0.29 during the three periods, respectively. The N-SAD index was highest in Wyoming, with values of 0.37, 0.41, and 0.41 during these periods, respectively. With respect to the positive sentiment index (P-SAD), during the initial outbreak period, it displayed a range from 0.42 (Montana) to 0.50 (Vermont). In the rapid spread period, the P-SAD index exhibited variations ranging from 0.39 (Wyoming) to 0.48 (Nebraska), while during the full-blown period, it spanned from 0.39 (Montana) to 0.49 (Hawaii). The Twitter user sentiment within Vermont consistently reflected a more optimistic outlook toward the pandemic, while users in Wyoming generally expressed a more pessimistic sentiment.

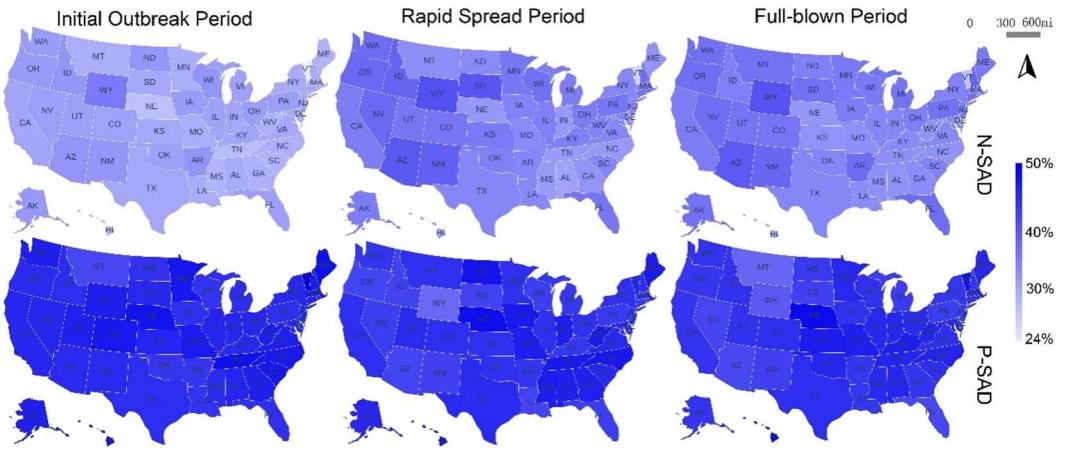

Figure 6. Spatiotemporal disparities of public sentiment toward COVID-19.

5.3. Model performance and time lag effects

In this study, we set the feature X_m to be SI, driving, transit, walking, RAD, negative, and positive and set the outcome Y_m to be the COVID-19 case rate, for each state m $\in \{1, \ldots, 50\}$ in the United States. Note that the outcome Y_m has been standardized based on the population size. For hyper-parameter tuning, we used grid search with the following parameter grids: $S_\rho = (0.2,\ 0.4,\ 0.6,\ 0.8)$, $S_S = (3, 4, 5, 6, 8, 10, 12)$, $S_\varrho = (0.1,\ 0.2,\ 0.4,\ 0.6,\ 0.8,\ 0.9)$, $S_\lambda = \left(0,\ \frac{\pi}{2}, \pi\right)$. The optimal choices of tuning parameters were obtained by applying Algorithm 1.

Meanwhile, we introduced temporal lag effects into the BSTS model, denoting this enhanced version as the BSTS-TL model. BSTS-TL model serves as the baseline model to assess the efficacy of the newly designed MBSTS-TL model. Please note that the MBSTS model is a special case of the MBSTS-TL model, so we do not use the MBSTS model as a baseline. We subsequently present a comparative evaluation of the modeling performance of both the BSTS-TL and MBSTS-TL models for three periods (the initial outbreak period, the rapid spread period, and the full-blown period), considering no time lag, 1-week lag, and 2-weeks lag effects through the year, i.e. $l_t = (0,\ 1,\ 2)$.

Table 2 reports the normalized absolute error (Equation 8) generated by the BSTS-TL model across different time lag selections and different pandemic phases. During the initial outbreak period, the normalized absolute errors range from 0.188 to 0.194, while in the rapid spread period, they range from 0.067 to 0.074. In the full-blown period, the normalized absolute errors range from 0.084 to 0.103. The average normalized absolute errors for time lags of 0, 1, and 2 weeks are 0.116, 0.115, and 0.117, respectively. As indicated in Table 3, the MBSTS-TL model demonstrates much smaller average normalized absolute errors across all three-time lag selections. Specifically, the average normalized absolute errors for time lags of 0, 1, and 2 weeks are 0.044, 0.047, and 0.051, respectively. During the initial outbreak period, the normalized absolute errors range from 0.016 to 0.023. In the rapid spread period, they range from 0.017 to 0.019, and in the full-blown period, they range from 0.097 to 0.111.

Table 2. The normalized absolute error (7) in different time lags in the BSTS-TL model.

Time lag (week)	The initial outbreak period	The rapid spread period	The full-blown period	Average
$l_t = 0$	0.194	0.074	0.084	0.116
$l_t = 1$	0.188	0.067	0.091	0.115
$l_t = 2$	0.194	0.067	0.091	0.117

Table 3. The normalized absolute error (7) in different time lags in the MBSTS-TL model.

Time lag (week)	The initial outbreak period	The rapid spread period	The full-blown period	Average
$l_t = 0$	0.016	0.018	0.097	0.044
$l_t = 1$	0.023	0.017	0.103	0.047
$l_t = 2$	0.022	0.019	0.111	0.051

Concurrently, the MBSTS-TL model demonstrates high accuracy during the initial outbreak and rapid spread periods, with consistently low normalized absolute errors. However, its performance is relatively less accurate during the full-blown period. This observation aligns with the reality that because human responses and COVID-19 spread in each region were highly volatile during this phase, the correlation becomes less significant comparatively in modeling.

Regarding the time lag selection in the MBSTS-TL Model, the smallest normalized absolute errors were observed when no time lag was considered during the initial outbreak and full-blown periods, yielding values of 0.016 and 0.097, respectively. In the rapid spread period, the inclusion of a one-week lag led to the smallest normalized absolute error of 0.017. These outcomes indicate the absence of time lag effects of human responses on the spread of COVID-19 during the initial outbreak and full-blown periods. In contrast, during the rapid spread period, changes in human responses appeared to impact the pandemic's spread one week later. Figure 7 portrays the spatiotemporal variation of normalized absolute errors in the MBSTS-TL Model at the state level during the three pandemic periods, considering 0-, 1-, and 2-week time lags. The recorded normalized absolute errors range from 0.00 to 0.31. The highest normalized absolute error emerged in Iowa (IA), North Carolina (NC), and New Mexico (NM) during the full-blown period, yielding respective values of 0.31, 0.30, and 0.29.

5.4. Modeled relationships and interpretation

Figure 8 depicts the coefficients of governmental and human responses derived from the MBSTS-TL model at the state level during three COVID-19 stages. The human response coefficients exhibited a range from −130.62 to 109.62, with positive coefficients depicted in red and negative coefficients in blue. These colors signify the positive and negative influences of human responses on COVID-19 spread, respectively. The saturation of colors reflects the absolute magnitudes of the coefficients, which indicate the degree of significance of human responses' impacts on the propagation of COVID-19.

Regarding the variations in the primary human responses influencing the spread of COVID-19 across distinct stages of the pandemic, our analysis identified human mobility in walking and driving as the two key factors impacting case rates in most states during the initial outbreak period. Notably, the coefficients associated with human mobility in walking and driving exhibited the most substantial absolute values across 22 and 13 states, respectively. In particular, the coefficients of human mobility

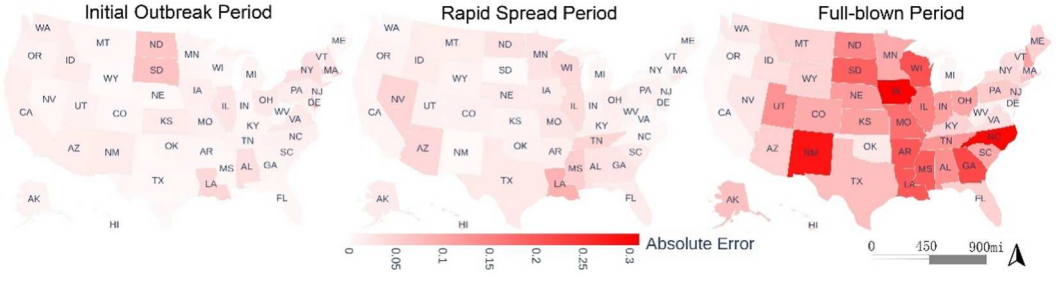

Figure 7. The normalized absolute error of the MBSTS-TL Model at the state level in three pandemic periods.

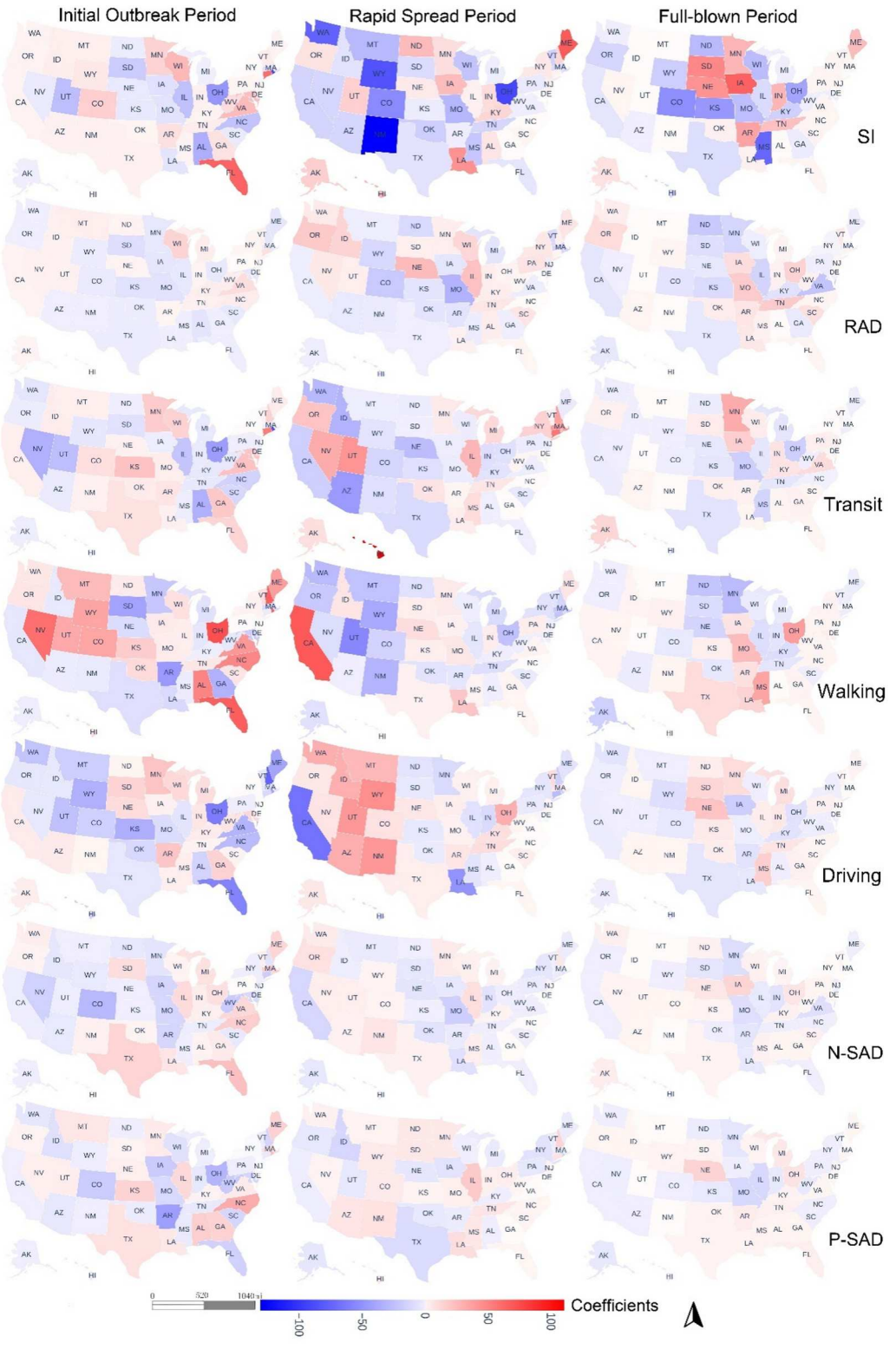

Figure 8. The spatial distribution of coefficients in three phases.

in walking ranged from 74.16 to 33.19 in a decreasing order of the states: Ohio, Florida, Nevada, Alabama, North Carolina, Virginia, Wyoming, Colorado, and Utah. This suggests that in these nine states, an increase in pedestrian movement intensified the COVID-19 outbreak. Conversely, in Arkansas, South Dakota, and Georgia, the coefficients of human mobility in walking ranged from −46.46 to −33.30 in increasing order, indicating that increases in pedestrian mobility alleviated COVID-19 transmission. Furthermore, in states such as New Hampshire, Maine, and Kansas, the coefficients of driving mobility varied from −75.97 to −35.81 in increasing order. These values highlight an association between decreased driving mobility and an uptick in COVID-19 case rates. Overall, the analysis emphasizes the intricate interplay between specific forms of human mobility and the dynamics of COVID-19 spread during different stages of the pandemic.

During the rapid spread period, the coefficients of SI and human mobility by transit displayed the highest absolute values across 20 and 15 states, respectively. Coefficients of SI were negative in five states – New Mexico, Ohio, Wyoming, Washington, and Colorado – ranging from −130.62 to −54.63 in increasing order. Conversely, in Maine, the coefficient of SI was 68.86, unfolding the positive impacts of stay-at-home policy strictness on the case rate change. Regarding human mobility by transiting, the coefficients were negative in Arizona (−45.98) and Idaho (−32.99), and positive in Hawaii, Connecticut, Massachusetts, New Hampshire, and Nevada, ranging from 109.62 to 32.28. It is worth mentioning that in California, human mobility in walking and driving were two principle human responses with coefficients of 69.52 and −67.78, respectively. These observations reveal that compared to the strictness of stay-at-home policies, the decrease in walking mobility and increment in driving mobility were more forceful human responses to the inhibition of COVID-19 in California.

Three human responses, i.e. stay-at-home policies, human mobility in walking, and public awareness toward COVID-19 served as the key factors of case rate evolving in 18, 10, and 9 states in the full-blown period, respectively. The more strictness of stay-at-home policies coincided with the dwindles of case rate change in Mississippi, Colorado, Kansas, Ohio, and North Dakota with the coefficients of SI ranging from −74.13 to −40.51 in an increasing order. Contrarily, the strictness of stay-at-home policies fostered positive impacts on COVID-19 spread in Iowa, South Dakota, Nebraska, and Arkansas, with the coefficients of SI ranging from 65.68 to 36.29. With respect to walking mobility, the coefficients were 14.61 in Louisiana, and −16.22 in Alaska, exhibiting the opposite impacts of walking mobility on COVID-19 control. The coefficients of RAD indexes were −22.73 in Virginia and −14.88 in Illinois, conveying that intensified public awareness of COVID-19 was the most pivotal human response for curving the COVID-19 spread in Virginia and Illinois in the full-blown period.

The results also showed that in Wisconsin, the stay-at-home policies consistently emerged as the most significant human responses affecting COVID-19 spread throughout the entire year. The coefficients of SI were 26.66, −23.59, and −27.44 in three pandemic periods, respectively. The impacts were positive in the initial outbreak period, and switched to negative in the following periods, depicting that the effectiveness of stay-at-home policies on COVID-19 control began in the rapid spread phase, and enhanced in the full-blown period in Wisconsin. Additionally, in Ohio, Colorado, Wyoming, Maine, South Dakota, Indiana, Hawaii, Kansas, Nebraska, and Arkansas, the COVID-19 spread was primarily shaped by the human mobility intensity in the initial outbreak period, and stay-at-home policies stand out as the most critical factor for COVID-19 control in the rapid spread and full-blown periods.

6. Discussion

6.1. Significant implications

This study has several significant implications. First, this study conducted a demographic-adjusted evaluation of two types of human responses encompassing public awareness (as measured by the

RAD index) and sentiments toward COVID-19 (captured by the N-SAD and P-SAD indexes). The human responses data set for COVID-19 in the U.S. at the state level for the year 2020 is readily accessible via a GitHub repository (https://github.com/yimindai0521/Replication_MBSTS_TL). This comprehensive human response data set serves as a fundamental resource for prospective investigations pertaining to societal resilience, ethical considerations within the domain of public health interventions, and the development of adaptable strategies for managing global health crises before pharmaceutical interventions become available.

Second, this study designed the MBSTS-TL model and applied it to address the high-dimensional challenges in spatiotemporal modelings using the COVID-19 spread as a case study. The MBSTS-TL model offers three distinctive advantages. The model incorporates considerations of spatial dependency and the impact of time lags when examining the relationships between various factors and the target time series. It also leverages the benefits of feature selection to estimate associations within high-dimensional time series. Furthermore, the model effectively addresses concerns related to overfitting when dealing with complex relationships. The MBSTS-TL model serves as a robust analytical instrument for conducting scenario analyses, enabling the evaluation of diverse intervention strategies and their potential consequences on pandemic outcomes. Owing to these inherent advantages, it is also well-suited for elucidating the intricate interplay among societal, economic, environmental, and other public health factors across a wide spectrum of contexts.

Finally, this study unveiled a dynamic pattern in the human responses influencing the spread of COVID-19 over various phases. The initial outbreak phase was predominantly driven by human mobility. During the subsequent rapid spread phase, it became evident that the stringency of policies assumed a pivotal role alongside mobility in shaping the pandemic's trajectory. As the pandemic entered its full-blown phase, the significance of public awareness regarding COVID-19 in influencing its progression emerged. This observed pattern underscores the critical importance of adopting a multifaceted strategy that incorporates measures related to mobility constraints, policy stringency, and the implementation of robust public awareness campaigns. The findings of ever-changing determinants that underlie pandemic propagation hold valuable implications for future pandemic preparedness. This emphasizes the necessity for phased and adaptive intervention strategies to achieve sustainable Good Health and Well-being (Goal 3) and Sustainable Cities and Communities (Goal 11) of the Sustainable Development Goals (SDGs).

6.2. Limitations

While the proposed framework in this study effectively addresses a majority of challenges in estimating the compounding impacts of governmental and human responses on the pandemic's health outcomes, it is important to acknowledge several limitations that warrant further investigation.

Accurate estimates of COVID-19 case counts and governmental and human responses are crucial for modeling and understanding their relationship. However, data uncertainty poses significant challenges in capturing governmental and human responses and the spread of the virus. In the U.S., COVID-19 confirmed case counts were underestimated, primarily due to limited test availability and imperfect test sensitivity, especially during early 2020. Wu et al. (2020) pointed out that a substantial number of mild or asymptomatic infections in the U.S. may have gone undetected, as the U.S. Centers for Disease Control and Prevention (CDC) prioritized testing hospitalized patients who tend to exhibit moderate to severe symptoms. Meanwhile, COVID-19 tests based on nasopharyngeal and throat swabs may produce false negative results, leading to the underestimation of COVID-19 cases. To achieve a more accurate understanding of the relationship between human responses and pandemic controls, a more realistic tracking and assessment of COVID-19 and future infectious disease cases is necessary. Uncertainty also exists in the Apple human mobility data, which only records the movement of people using Apple Maps and does not provide a comprehensive representation of overall human mobility. Movements of individuals without GPS-enabled devices or those using different mapping apps cannot be captured in this data. To enhance

mobility tracking, it is imperative to incorporate additional human mobility data sources, such as Google human mobility data and SafeGraph data sets.

The concept of 'scales of analysis' has long been a geospatial matter that has not yet been systematically elucidated. This term alludes to the level or perspective at which a problem or issue is examined or addressed, encompassing a spectrum from the global level down to the individual level (Watson 1978). The choice of analysis scale is contingent upon the scale of the problems or issues under consideration. While the COVID-19 pandemic unfolds at the global level, the transmission of the virus is intricately connected to individual interactions. The human responses and the spread of COVID-19 highlight spatial disparities across various countries, states, counties, and even communities. Similarly, temporal scales are essential for understanding the pandemic's progression and its responses. In this study, we divided the pandemic into three phases, reflecting key stages of viral spread and response patterns across the United States. This temporal classification allowed us to identify broad patterns while ensuring sufficient data for model training. However, this three-phase framework may oversimplify the pandemic's complexities, as regions experienced different surges and response timings. A more granular temporal analysis could reveal these variations in greater detail. Additionally, due to limitations in the availability of quantitative data concerning COVID-19-related policies, this study is confined to the state level, treating each state as a single entity and thereby overlooking the spatial heterogeneity in the effects of human responses on COVID-19 with each state. In future research, conducting finer-scale analyses – both spatially (moving from state to city-level or neighborhood-level) and temporally (dividing the pandemic into more phases considering local patterns) – could provide a more nuanced understanding of the interplay between human responses and the spread of COVID-19.

Moreover, the influence of human responses on the dissemination of COVID-19 is contingent upon various localized factors, such as population density, the influx of individuals from initial outbreak epicenters, and prevailing mobility patterns. Additionally, human behaviors during health crises are shaped by factors such as trust in government, media influence, cultural norms, and the use of technological tools like contract tracing or health monitoring apps. Incorporating these elements in future research can enhance our understanding of why people across different regions, stages, and cultural contexts with various tools respond uniquely to pandemics from a behavioral science perspective.

7. Conclusion

This study collected Twitter data, COVID-19 case rates, Apple human mobility data, and the stringency of stay-at-home policies in the U.S. during the year 2020. The contributions of this work are two-fold. Initially, it elucidates the spatiotemporal disparities in human responses, encompassing aspects such as public awareness and sentiment towards COVID-19, human mobility patterns, and the rigor of COVID-19 policies, within the U.S. throughout 2020. We introduced the RAD index to estimate demographically adjusted public awareness towards COVID-19 using Twitter data. We also produced weekly N-SAD and P-SAD indices at the state level, quantitatively capturing negative and positive public sentiment regarding COVID-19 based on Twitter data. Second, it designs and employs a statistical machine learning model, MBSTS-TL, for the comprehensive modeling of the cumulative effects of governmental and human responses on COVID-19 health outcomes, with a specific emphasis on accounting for spatial interdependencies and temporal lag effects in the relationships. The MBSTS-TL model uncovered interconnected relationships between governmental and human responses and COVID-19 health outcomes while considering spatial dependencies and the time lag effects of governmental and human responses on the transmission of COVID-19.

The research outcomes have yielded significant insights. First, it has unveiled spatiotemporal discrepancies in governmental and human responses pertaining to COVID-19 in the U.S. at the state level. Nationally, during the initial outbreak period (from week 9 to week 22, spanning from late

February to the end of May), public awareness experienced a rapid increase, reaching a significant peak. Sentiment towards COVID-19 reflected on social media were most negative during this period compared to the remainder of 2020. The stringency of stay-at-home policies also increased rapidly and remained at a relatively stringent level. Human mobility, whether by walking, driving, or transit, witnessed varying degrees of decline and recovery. At the state level, human responses displayed temporal and geographical variations. For instance, Louisiana consistently exhibited lower levels of public awareness about the pandemic among Twitter users throughout 2020, while Twitter users in Vermont consistently demonstrated a more optimistic outlook regarding the pandemic, and those in Wyoming generally expressed a more pessimistic sentiment. Second, the developed MBSTS-TL model demonstrated satisfactory accuracy in modeling the pandemic spread during the initial outbreak and rapid spread periods, with consistently low normalized absolute errors. The findings of the MBSTS-TL model indicated a shift in the determinants of COVID-19 health impacts over time, transitioning from an emphasis on human mobility during the initial outbreak period to a combination of human mobility and stay-at-home policies during the rapid spread period, and eventually involving human mobility, stay-at-home policies, and public awareness towards COVID-19 in the full-blown phase.

The human responses data set and the proposed MBSTS-TL model offer valuable insights for diverse applications. The human responses data set provides a valuable resource for social scientists aiming to comprehend the dynamics of human activities across space and time during the pandemic. The MBSTS-TL model can be effectively employed to unveil complex interrelationships within human-public health systems and human-environment dynamics. The results identify the evolving determinants of human responses to pandemic spread, offering guidance to policymakers for designing and implementing phased and adaptive strategies. These evidence-based solutions can help mitigate the adverse impacts of future pandemics and develop sustainable pandemic-resilient cities.

Acknowledgements

Any opinions, findings, conclusions, or recommendations expressed in this material are those of the authors and do not necessarily reflect the views of the funding agencies.

Disclosure statement

No potential conflict of interest was reported by the author(s).

Funding

This study is supported by three grants, including the Data Resource Develop Program Award from the Texas A\&M Institute of Data Science (TAMIDS), the Seed Fund Award from the College of Arts\& Sciences at Texas A\&M University, and the U.S. National Science Foundation – Collaborative Research: HNDS-I: Cyberinfrastructure for Human Dynamics and Resilience Research (Award No. 2318206). The research of N.N. was partially supported by NIH grant 1R21AI180492-01 and the Individual Research Grant at Texas A\&M University.

Data availability statement

The data used in this research were derived from the following resources available in the public domain: Twitter Application Programming Interface (API) for Academic Research (https://developer.twitter.com/en/products/twitter-api/academic-research), Oxford Covid-19 Government Response Tracker (OxCGRT) (https://github.com/OxCGRT/covid-policy-tracker#oxford-covid-19-government-response-tracker-oxcgrt), and COVID-19 Data Repository by the Center for Systems Science and Engineering (CSSE) at Johns Hopkins University (https://github.com/CSSEGISandData/COVID-19). The RAD, N-SAD, and P-SAD dataset, as well as the Replication code and mbsts-tl function generated in this study, are available as a GitHub repository (https://github.com/yimindai0521/Replication_MBSTS_TL).

References

Agusto, Folashade B., Eric Numfor, Karthik Srinivasan, Enahoro A. Iboi, Alexander Fulk, Jarron M. Saint Onge, and A. Townsend Peterson. 2023. "Impact of Public Sentiments on the Transmission of COVID-19 Across a Geographical Gradient." *PeerJ* 11 (February): e14736. https://doi.org/10.7717/peerj.14736.

Ak, Çiğdem, Alex D. Chitsazan, Mehmet Gönen, Ruth Etzioni, and Aaron J. Grossberg. 2022. "Spatial Prediction of COVID-19 Pandemic Dynamics in the United States." *ISPRS International Journal of Geo-Information* 11 (9): 470. https://doi.org/10.3390/ijgi11090470.

Alqurashi, Sarah, Ahmad Alhindi, and Eisa Alanazi. 2020. "Large Arabic Twitter Dataset on COVID-19." arXiv. https://doi.org/10.48550/arXiv.2004.04315.

Altmann, M. 1995. "Susceptible-Infected-Removed Epidemic Models with Dynamic Partnerships." *Journal of Mathematical Biology* 33 (6): 661–675. https://doi.org/10.1007/BF00298647.

Banda, Juan M., Ramya Tekumalla, Guanyu Wang, Jingyuan Yu, Tuo Liu, Yuning Ding, Ekaterina Artemova, Elena Tutubalina, and Gerardo Chowell. 2021. "A Large-Scale COVID-19 Twitter Chatter Dataset for Open Scientific Research – An International Collaboration." *Epidemiologia* 2 (3): 315–324. https://doi.org/10.3390/epidemiologia2030024.

Bhattacharya, A., and D. B. Dunson. 2011. "Sparse Bayesian Infinite Factor Models." *Biometrika* 98 (2): 291–306. https://doi.org/10.1093/biomet/asr013.

Blank, Grant. 2017. "The Digital Divide Among Twitter Users and Its Implications for Social Research." *Social Science Computer Review* 35 (6): 679–697. https://doi.org/10.1177/0894439316671698.

Bogdanowicz, Alexander, and ChengHe Guan. 2022. "Dynamic Topic Modeling of Twitter Data During the COVID-19 Pandemic." *PLoS One* 17 (5): e0268669. https://doi.org/10.1371/journal.pone.0268669.

Brodersen, Kay H., Fabian Gallusser, Jim Koehler, Nicolas Remy, and Steven L. Scott. 2015. "Inferring Causal Impact Using Bayesian Structural Time-Series Models." *The Annals of Applied Statistics* 9 (1): 247–274. https://doi.org/10.1214/14-AOAS788.

Burki, Talha. 2020. "China's Successful Control of COVID-19." *The Lancet Infectious Diseases* 20 (11): 1240–1241. https://doi.org/10.1016/S1473-3099(20)30800-8.

Chen, Yixiang, Min Chen, Bo Huang, Chao Wu, and Wenjia Shi. 2021. "Modeling the Spatiotemporal Association Between COVID-19 Transmission and Population Mobility Using Geographically and Temporally Weighted Regression." *GeoHealth* 5 (5): e2021GH000402. https://doi.org/10.1029/2021GH000402.

Chen, Chao, Tao Feng, and Xiaoning Gu. 2022. "Role of Latent Factors and Public Policies in Travel Decisions under COVID-19 Pandemic: Findings of a Hybrid Choice Model." *Sustainable Cities and Society* 78 (March): 103601. https://doi.org/10.1016/j.scs.2021.103601.

Chen, Yi-Cheng, Ping-En Lu, Cheng-Shang Chang, and Tzu-Hsuan Liu. 2020. "A Time-Dependent SIR Model for COVID-19 With Undetectable Infected Persons." *IEEE Transactions on Network Science and Engineering* 7 (4): 3279–3294. https://doi.org/10.1109/TNSE.2020.3024723.

Cinarka, Halit, Mehmet Atilla Uysal, Atilla Cifter, Elif Yelda Niksarlioglu, and Aslı Çarkoğlu. 2021. "The Relationship Between Google Search Interest for Pulmonary Symptoms and COVID-19 Cases Using Dynamic Conditional Correlation Analysis." *Scientific Reports* 11 (1): 14387. https://doi.org/10.1038/s41598-021-93836-y.

Clyde, Merlise, Giovanni Parmigiani, and Brani Vidakovic. 1998. "Multiple Shrinkage and Subset Selection in Wavelets." *Biometrika* 85 (2): 391–401. https://doi.org/10.1093/biomet/85.2.391.

Dainton, Christopher, and Alexander Hay. 2021. "Quantifying the Relationship Between Lockdowns, Mobility, and Effective Reproduction Number (Rt) During the COVID-19 Pandemic in the Greater Toronto Area." *BMC Public Health* 21 (1): 1658. https://doi.org/10.1186/s12889-021-11684-x.

Dlamini, Wisdom M. D., Sabelo P. Simelane, and Nhlanhla M. Nhlabatsi. 2022. "Bayesian Network-Based Spatial Predictive Modelling Reveals COVID-19 Transmission Dynamics in Eswatini." *Spatial Information Research* 30 (1): 183–194. https://doi.org/10.1007/s41324-021-00421-6.

Dong, Ensheng, Hongru Du, and Lauren Gardner. 2020. "An Interactive Web-Based Dashboard to Track COVID-19 in Real Time." *The Lancet Infectious Diseases* 20 (5): 533–534. https://doi.org/10.1016/S1473-3099(20)30120-1.

Durbin, J., and S. J. Koopman. 2002. "A Simple and Efficient Simulation Smoother for State Space Time Series Analysis." *Biometrika* 89 (3): 603–616. https://doi.org/10.1093/biomet/89.3.603.

Fotheringham, A. Stewart, Ricardo Crespo, and Jing Yao. 2015. "Geographical and Temporal Weighted Regression (GTWR)." *Geographical Analysis* 47 (4): 431–452. https://doi.org/10.1111/gean.12071.

Fu, Xinyu, and Wei Zhai. 2021. "Examining the Spatial and Temporal Relationship between Social Vulnerability and Stay-at-Home Behaviors in New York City during the COVID-19 Pandemic." *Sustainable Cities and Society* 67 (April): 102757. https://doi.org/10.1016/j.scs.2021.102757.

Galea, Sandro, Matthew Riddle, and George A Kaplan. 2010. "Causal Thinking and Complex System Approaches in Epidemiology." *International Journal of Epidemiology* 39 (1): 97–106. https://doi.org/10.1093/ije/dyp296.

Gao, Song, Jinmeng Rao, Yuhao Kang, Yunlei Liang, and Jake Kruse. 2020. "Mapping County-Level Mobility Pattern Changes in the United States in Response to COVID-19." *SIGSPATIAL Special* 12 (1): 16–26. https://doi.org/10.1145/3404820.3404824.

George, Edward I., and Robert E. McCulloch. 1997. "Approaches for Bayesian Variable Selection." *Statistica Sinica* 7 (2): 339–373.

Hadjidemetriou, Georgios M., Manu Sasidharan, Georgia Kouyialis, and Ajith K. Parlikad. 2020. "The Impact of Government Measures and Human Mobility Trend on COVID-19 Related Deaths in the UK." *Transportation Research Interdisciplinary Perspectives* 6 (July): 100167. https://doi.org/10.1016/j.trip.2020.100167.

Hafner, Christian M. 2020. "The Spread of the Covid-19 Pandemic in Time and Space." *International Journal of Environmental Research and Public Health* 17 (11): 3827. https://doi.org/10.3390/ijerph17113827.

Hale, Thomas, Noam Angrist, Rafael Goldszmidt, Beatriz Kira, Anna Petherick, Toby Phillips, Samuel Webster, et al. 2021. "A Global Panel Database of Pandemic Policies (Oxford COVID-19 Government Response Tracker)." *Nature Human Behaviour* 5 (4): 529–538. https://doi.org/10.1038/s41562-021-01079-8.

Hatami, Faizeh, Shi Chen, Rajib Paul, and Jean-Claude Thill. 2022. "Simulating and Forecasting the COVID-19 Spread in a U.S. Metropolitan Region with a Spatial SEIR Model." *International Journal of Environmental Research and Public Health* 19 (23): 15771. https://doi.org/10.3390/ijerph192315771.

Hou, Xiao, Song Gao, Qin Li, Yuhao Kang, Nan Chen, Kaiping Chen, Jinmeng Rao, Jordan S. Ellenberg, and Jonathan A. Patz. 2021. "Intracounty Modeling of COVID-19 Infection with Human Mobility: Assessing Spatial Heterogeneity with Business Traffic, Age, and Race." *Proceedings of the National Academy of Sciences* 118 (24): e2020524118. https://doi.org/10.1073/pnas.2020524118.

Ionides, Edward L., Ning Ning, and Jesse Wheeler. 2022. "An Iterated Block Particle Filter for Inference on Coupled Dynamic Systems with Shared and Unit-Specific Parameters." arXiv. https://doi.org/10.48550/arXiv.2206.03837.

Jammalamadaka, S. R., J. Qiu, and N. Ning. 2019. "Predicting a Stock Portfolio with the Multivariate Bayesian Structural Time Series Model: Do News or Emotions Matter?" *International Journal of Artificial Intelligence* 17 (2): 81–104.

Jun, Seung-Pyo, Hyoung Sun Yoo, and Jae-Seong Lee. 2021. "The Impact of the Pandemic Declaration on Public Awareness and Behavior: Focusing on COVID-19 Google Searches." *Technological Forecasting and Social Change* 166 (May): 120592. https://doi.org/10.1016/j.techfore.2021.120592.

Kim, Honghyok, Antonella Zanobetti, and Michelle L. Bell. 2021. "Temporal Transition of Racial/Ethnic Disparities in COVID-19 Outcomes in 3108 Counties of the United States: Three Phases from January to December 2020." *The Science of the Total Environment* 791 (October): 148167. https://doi.org/10.1016/j.scitotenv.2021.148167.

Kraemer, Moritz U. G., Chia-Hung Yang, Bernardo Gutierrez, Chieh-Hsi Wu, Brennan Klein, David M. Pigott, et al. 2020. "The Effect of Human Mobility and Control Measures on the COVID-19 Epidemic in China." *Science* 368 (6490): 493–497. https://doi.org/10.1126/science.abb4218.

Kurita, Junko, Yoshiyuki Sugishita, Tamie Sugawara, and Yasushi Ohkusa. 2021. "Evaluating Apple Inc Mobility Trend Data Related to the COVID-19 Outbreak in Japan: Statistical Analysis." *JMIR Public Health and Surveillance* 7 (2): e20335. https://doi.org/10.2196/20335.

Li, Ruiyun, Sen Pei, Bin Chen, Yimeng Song, Tao Zhang, Wan Yang, and Jeffrey Shaman. 2020. "Substantial Undocumented Infection Facilitates the Rapid Dissemination of Novel Coronavirus (SARS-CoV-2)." *Science* 368 (6490): 489–493. https://doi.org/10.1126/science.abb3221.

Li, Weiyu, Qi Wang, Yuanyuan Liu, Mario L. Small, and Jianxi Gao. 2022. "A Spatiotemporal Decay Model of Human Mobility When Facing Large-Scale Crises." *Proceedings of the National Academy of Sciences* 119 (33): e2203042119. https://doi.org/10.1073/pnas.2203042119.

Lin, Binbin, Lei Zou, Nick Duffield, Ali Mostafavi, Heng Cai, Bing Zhou, Jian Tao, Mingzheng Yang, Debayan Mandal, and Joynal Abedin. 2022. "Revealing the Linguistic and Geographical Disparities of Public Awareness to Covid-19 Outbreak through Social Media." *International Journal of Digital Earth* 15 (1): 868–889. https://doi.org/10.1080/17538947.2022.2070677.

Lin, Binbin, Lei Zou, Mingzheng Yang, Bing Zhou, Debayan Mandal, Joynal Abedin, Heng Cai, and Ning Ning. 2024a. "Progress in Understanding Human-COVID-19 Dynamics Using Geospatial Big Data: A Systematic Review." *Annals of GIS* 0 (0): 1–21. https://doi.org/10.1080/19475683.2024.2418584.

Lin, Binbin, Lei Zou, Bo Zhao, Xiao Huang, Heng Cai, Mingzheng Yang, and Bing Zhou. 2024b. "Sensing the Pulse of the Pandemic: Unveiling the Geographical and Demographic Disparities of Public Sentiment Toward COVID-19 Through Social Media." *Cartography and Geographic Information Science* 51 (3): 366–384. https://doi.org/10.1080/15230406.2024.2323489.

Liu, Yang, Christian Morgenstern, James Kelly, Rachel Lowe, James Munday, C. Julian Villabona-Arenas, Hamish Gibbs, et al. 2021. "The Impact of Non-Pharmaceutical Interventions on SARS-CoV-2 Transmission Across 130 Countries and Territories." *BMC Medicine* 19 (1): 40. https://doi.org/10.1186/s12916-020-01872-8.

Ma, Zihui, Lingyao Li, Libby Hemphill, Gregory B. Baecher, and Yubai Yuan. 2024. "Investigating Disaster Response for Resilient Communities through Social Media Data and the Susceptible-Infected-Recovered (SIR) Model: A Case Study of 2020 Western U.S. Wildfire Season." *Sustainable Cities and Society* 106 (July): 105362. https://doi.org/10.1016/j.scs.2024.105362.

Madigan, David, and Adrian E. Raftery. 1994. "Model Selection and Accounting for Model Uncertainty in Graphical Models Using Occam's Window." *Journal of the American Statistical Association* 89 (428): 1535–1546. https://doi.org/10.1080/01621459.1994.10476894.

Manzira, Christopher K, Anna Charly, and Brian Caulfield. 2022. "Assessing the Impact of Mobility on the Incidence of COVID-19 in Dublin City." *Sustainable Cities and Society* 80 (May): 103770. https://doi.org/10.1016/j.scs.2022.103770.

Morgan-Lopez, Antonio A., Annice E. Kim, Robert F. Chew, and Paul Ruddle. 2017. "Predicting Age Groups of Twitter Users Based on Language and Metadata Features." *PLoS One* 12 (8): e0183537. https://doi.org/10.1371/journal.pone.0183537.

Nagy, Benedek, Rozalia Gabor Manuela, Bacoș Ioan-Bogdan, Kabil Moaaz, Zhu Kai, and Dénes Dávid Lóránt. 2023. "Google and Apple Mobility Data as Predictors for European Tourism During the COVID-19 Pandemic: A Neural Network Approach." *Equilibrium. Quarterly Journal of Economics and Economic Policy* 18 (2): 419–459.

Ning, Ning, and Edward L. Ionides. 2023. "Iterated Block Particle Filter for High-Dimensional Parameter Learning: Beating the Curse of Dimensionality." *Journal of Machine Learning Research* 24 (82): 1–76.

Ning, Yu-Chien Bo, and Ning Ning. 2024. "Spike and Slab Bayesian Sparse Principal Component Analysis." *Statistics and Computing* 34 (3): 118. https://doi.org/10.1007/s11222-024-10430-8.

Ning, Ning, and Jinwen Qiu. 2023. "The Mbsts Package: Multivariate Bayesian Structural Time Series Models in R." arXiv. http://arxiv.org/abs/2106.14045.

Pati, Debdeep, Anirban Bhattacharya, Natesh S. Pillai, and David Dunson. 2014. "Posterior Contraction in Sparse Bayesian Factor Models for Massive Covariance Matrices." *The Annals of Statistics* 42 (3): 1102–1130. https://doi.org/10.1214/14-AOS1215.

Qiu, Jinwen, S. Rao Jammalamadaka, and Ning Ning. 2018. "Multivariate Bayesian Structural Time Series Model." *Journal of Machine Learning Research* 19 (68): 1–33.

Qiu, Jinwen, S. Rao Jammalamadaka, and Ning Ning. 2020. "Multivariate Time Series Analysis from a Bayesian Machine Learning Perspective." *Annals of Mathematics and Artificial Intelligence* 88 (10): 1061–1082. https://doi.org/10.1007/s10472-020-09710-6.

Rovetta, Alessandro, and Akshaya Srikanth Bhagavathula. 2020. "COVID-19-Related Web Search Behaviors and Infodemic Attitudes in Italy: Infodemiological Study." *JMIR Public Health and Surveillance* 6 (2): e19374. https://doi.org/10.2196/19374.

Scott, Steven L., and Hal R. Varian. 2014. "Predicting the Present with Bayesian Structural Time Series." *International Journal of Mathematical Modelling and Numerical Optimisation* 5 (1–2): 4–23. https://doi.org/10.1504/IJMMNO.2014.059942.

Subramanian, Rahul, Qixin He, and Mercedes Pascual. 2021. "Quantifying Asymptomatic Infection and Transmission of COVID-19 in New York City Using Observed Cases, Serology, and Testing Capacity." *Proceedings of the National Academy of Sciences* 118 (9): e2019716118. https://doi.org/10.1073/pnas.2019716118.

Sugiyama, Masashi. 2015. *Introduction to Statistical Machine Learning*. Waltham, MA: Morgan Kaufmann.

Sung, Hyungun. 2023. "Causal Impacts of the COVID-19 Pandemic on Daily Ridership of Public Bicycle Sharing in Seoul." *Sustainable Cities and Society* 89 (February): 104344. https://doi.org/10.1016/j.scs.2022.104344.

Tibshirani, Robert. 1996. "Regression Shrinkage and Selection Via the Lasso." *Journal of the Royal Statistical Society: Series B (Methodological)* 58 (1): 267–288. https://doi.org/10.1111/j.2517-6161.1996.tb02080.x.

Tsao, Shu-Feng, Helen Chen, Therese Tisseverasinghe, Yang Yang, Lianghua Li, and Zahid A. Butt. 2021. "What Social Media Told Us in the Time of COVID-19: A Scoping Review." *The Lancet Digital Health* 3 (3): e175–e194. https://doi.org/10.1016/S2589-7500(20)30315-0.

Vashisth, Pradeep, and Kevin Meehan. 2020. "Gender Classification Using Twitter Text Data." In *2020 31st Irish Signals and Systems Conference (ISSC)*, 1–6. https://doi.org/10.1109/ISSC49989.2020.9180161.

Vinceti, Marco, Tommaso Filippini, Kenneth J. Rothman, Fabrizio Ferrari, Alessia Goffi, Giuseppe Maffeis, and Nicola Orsini. 2020. "Lockdown Timing and Efficacy in Controlling COVID-19 Using Mobile Phone Tracking." *eClinicalMedicine* 25 (August): 1–7. https://doi.org/10.1016/j.eclinm.2020.100457.

Wang, Zijian, Scott Hale, David Ifeoluwa Adelani, Przemyslaw Grabowicz, Timo Hartman, Fabian Flöck, and David Jurgens. 2019. "Demographic Inference and Representative Population Estimates from Multilingual Social Media Data." In *The World Wide Web Conference, 2056–2067. WWW '19*. New York, NY: Association for Computing Machinery.

Wangping, Jia, Han Ke, Song Yang, Cao Wenzhe, Wang Shengshu, Yang Shanshan, Wang Jianwei, et al. 2020. "Extended SIR Prediction of the Epidemics Trend of COVID-19 in Italy and Compared With Hunan, China." *Frontiers in Medicine* 7 (May): 1–7. https://doi.org/10.3389/fmed.2020.00169

Watson, Mary K. 1978. "The Scale Problem in Human Geography." *Geografiska Annaler: Series B, Human Geography* 60 (1): 36–47. https://doi.org/10.1080/04353684.1978.11879429.

Wellenius, Gregory A., Swapnil Vispute, Valeria Espinosa, Alex Fabrikant, Thomas C. Tsai, Jonathan Hennessy, Andrew Dai, et al. 2021. "Impacts of Social Distancing Policies on Mobility and COVID-19 Case Growth in the US." *Nature Communications* 12 (1): 3118. https://doi.org/10.1038/s41467-021-23404-5.

Wong, David W. S., and Yun Li. 2020. "Spreading of COVID-19: Density Matters." *PLoS One* 15 (12): e0242398. https://doi.org/10.1371/journal.pone.0242398.

Wu, Sean L., Andrew N. Mertens, Yoshika S. Crider, Anna Nguyen, Nolan N. Pokpongkiat, Stephanie Djajadi, Anmol Seth, et al. 2020. "Substantial Underestimation of SARS-CoV-2 Infection in the United States." *Nature Communications* 11 (1): 4507. https://doi.org/10.1038/s41467-020-18272-4.

Wu, Jianyong, and Shuying Sha. 2021. "Pattern Recognition of the COVID-19 Pandemic in the United States: Implications for Disease Mitigation." *International Journal of Environmental Research and Public Health* 18 (5): 2493. https://doi.org/10.3390/ijerph18052493.

Zhang, Yunchang, and Jon D. Fricker. 2021. "Quantifying the Impact of COVID-19 on Non-Motorized Transportation: A Bayesian Structural Time Series Model." *Transport Policy* 103 (March): 11–20. https://doi.org/10.1016/j.tranpol.2021.01.013.

Zou, Hui, and Trevor Hastie. 2005. "Regularization and Variable Selection Via the Elastic Net." *Journal of the Royal Statistical Society Series B: Statistical Methodology* 67 (2): 301–320. https://doi.org/10.1111/j.1467-9868.2005.00503.x.

Zou, Hui, Trevor Hastie, and Robert Tibshirani. 2006. "Sparse Principal Component Analysis." *Journal of Computational and Graphical Statistics* 15 (2): 265–286. https://doi.org/10.1198/106186006X113430.

Zou, Lei, Nina S. N. Lam, Shayan Shams, Heng Cai, Michelle A. Meyer, Seungwon Yang, Kisung Lee, Seung-Jong Park, and Margaret A. Reams. 2019. "Social and Geographical Disparities in Twitter Use during Hurricane Harvey." *International Journal of Digital Earth* 12 (11): 1300–1318. https://doi.org/10.1080/17538947.2018.1545878.